

1 Identification of proteotoxic and proteoprotective bacteria that non-specifically affect proteins  
2 associated with neurodegenerative diseases

3  
4 Alyssa C Walker<sup>1</sup>, Rohan Bhargava<sup>1</sup>, Michael Bucher<sup>1</sup>, Amanda S Brust<sup>1</sup>, Daniel M Czyż<sup>1\*</sup>  
5 <sup>1</sup>Department of Microbiology and Cell Science, University of Florida, Gainesville, FL 32611,  
6 USA

7 \*Correspondence: [dczyz@ufl.edu](mailto:dczyz@ufl.edu)

## 8 9 **Summary**

10 Neurodegenerative protein conformational diseases (PCDs), such as Alzheimer's, Parkinson's,  
11 and Huntington's, are a leading cause of death and disability worldwide and have no known  
12 cures or effective treatments. Emerging evidence suggests a role for the gut microbiota in the  
13 pathogenesis of neurodegenerative PCDs; however, the influence of specific bacteria on the  
14 culprit proteins associated with each of these diseases remains elusive, primarily due to the  
15 complexity of the microbiota. In the present study, we employed a single-strain screening  
16 approach to identify human bacterial isolates that enhance or suppress the aggregation of culprit  
17 proteins and the associated toxicity in *Caenorhabditis elegans* expressing A $\beta$ <sub>1-42</sub>,  $\alpha$ -synuclein,  
18 and polyglutamine tracts. Here, we reveal the first comprehensive analysis of the human  
19 microbiome for its effect on proteins associated with neurodegenerative diseases. Our results  
20 suggest that bacteria affect the aggregation of metastable proteins by modulating host  
21 proteostasis rather than selectively targeting specific disease-associated proteins. These results  
22 reveal bacteria that potentially influence the pathogenesis of PCDs and open new promising  
23 prevention and treatment opportunities by altering the abundance of beneficial and detrimental  
24 microbes.

## 25 26 **Introduction**

27 Neurodegenerative protein conformational diseases (PCDs) are characterized by disturbances in  
28 proteostasis that result in the aggregation of disease-associated proteins, ultimately leading to  
29 tissue death.<sup>1</sup> Alzheimer's disease (AD), Parkinson's disease (PD), Huntington's disease (HD),  
30 and amyotrophic lateral sclerosis (ALS) are among the most prevalent neurodegenerative  
31 diseases, with AD recognized by the World Health Organization (WHO) as one of the leading  
32 causes of death worldwide.<sup>2</sup> However, despite their increasing prevalence, the etiology and  
33 potential therapeutic targets remain obscure. The sporadic onset and variable severity of  
34 neurodegenerative diseases, along with their idiopathic nature, suggest the possibility of a  
35 triggering factor for their onset and progression. Multiple factors have been associated with the  
36 pathogenicity of PCDs, including an expanding body of evidence that suggests the involvement  
37 of microbes, but primarily those within the human gut microbiota (HGM). The HGM is  
38 considered an "organ" due to its production of essential proteins and metabolites, including  
39 vitamins, hormones, and neurotransmitters.<sup>3,4</sup> Hence, dysbiosis of the gut microbiota has been  
40 linked to various ailments, including neurodegenerative diseases.<sup>5</sup>

41  
42 The complexity of the microbiome has made it challenging to determine the precise role of  
43 bacteria in the pathogenesis of neurodegenerative diseases. In addition, most of the evidence that  
44 associates bacteria with the occurrence of neurodegenerative diseases is based on correlation.<sup>6</sup>  
45 Interestingly, correlational evidence does not demonstrate any selectivity between different  
46 neurodegenerative diseases, despite each disease featuring a unique, specific culprit protein

47 species. For example, a lower abundance of *Prevotella* spp. has been observed in patients with  
48 different PCDs, including PD, and ALS.<sup>7-15</sup> Due to this lack of specificity, we hypothesized that  
49 bacteria could be affecting these diseases through the host proteostasis network—upstream of  
50 protein aggregate formation. This hypothesis is further supported by our previous study in which  
51 we identified gram-negative enteropathogens that significantly disrupt proteostasis across tissues  
52 in *C. elegans*.<sup>16</sup> The utility of *C. elegans* as a model to study host-microbe interaction is  
53 strengthened by its unique ability to be colonized by a single bacterial strain. Such a feature  
54 simplifies the complexity of the microbiome, allowing us to study the effect of individual species  
55 on host proteostasis.

56  
57 Here, we characterized the effect of 229 unique bacterial isolates from the Human Microbiome  
58 Project on the aggregation of disease-associated proteins in *C. elegans*, using transgenic  
59 nematodes expressing A $\beta$ <sub>1-42</sub>,  $\alpha$ -synuclein, and polyglutamine (PolyQ). Surprisingly, our results  
60 suggest that bacteria-mediated enhancement or suppression of host protein aggregation is not  
61 specific to any particular culprit protein species. Instead, our results demonstrate that bacteria  
62 broadly affect the aggregation of metastable proteins present within the host proteome.  
63 Furthermore, we also observed that the proteostasis-modulating effects of intestinal bacteria  
64 reach distal tissues. Thus, our results indicate that bacteria influence host proteostasis, ultimately  
65 affecting the ability of both proximal and distal tissues to buffer protein folding. To date, our  
66 results provide the most comprehensive characterization of the effect of individual constituents  
67 of the human microbiome on host proteostasis. These results reveal the bacterial contribution to  
68 the pathogenesis of AD, PD, HD, ALS, and possibly other PCDs. Collectively, our results  
69 provide a framework for the development of microbiome-based risk factor assessments and  
70 disease management strategies.

## 71 **Results**

### 72 **Characterization of the human microbiome on host proteostasis**

73 We obtained a comprehensive Human Microbiome Project collection of 229 unique bacterial  
74 isolates from BEI Resources and assessed their effect on *C. elegans* proteostasis. The method  
75 used to conduct this experiment is illustrated in Figure 1. The collection encompasses isolates  
76 from a range of diverse phyla and a variety of anatomical sites (Figure 2). In our previous study,  
77 we used aggregation-prone polyQ tracts as a sensor of the protein folding environment to  
78 demonstrate that gram-negative pathogens disrupt host proteostasis.<sup>16</sup> Among animals carrying  
79 intestine-, muscle-, and neuron-specific polyQ::YFP, we previously found that proteostasis in the  
80 intestine was most robustly affected by the colonizing bacteria.<sup>16</sup> As such, we performed our  
81 initial screen using the intestinal polyQ model (Figure 2). To eliminate the possibility that  
82 bacteria will affect *C. elegans* development, worms were grown to adulthood prior to being  
83 transferred to the bacterial strains of interest. polyQ aggregation was assessed by fluorescent  
84 microscopy. To ensure the validity of our results, we also assessed polyQ aggregation by western  
85 blotting. Validating our approach, both quantitative methods yielded similar results.

86  
87  
88 [Place **Figure 1** here]

89  
90 Bacteria from the isolate collection exhibited a differential effect on *C. elegans* proteostasis as  
91 indicated by increases and decreases in polyQ aggregation compared to worms fed control *E.*  
92 *coli* OP50 (Figure 2). Figure 2 summarizes the screen revealing bacteria that most robustly

93 affected host proteostasis. For example, *Prevotella* was the only genus that consistently resulted  
94 in low polyQ aggregation across all 229 strains tested (Figure 2). Conversely, significant host  
95 proteotoxicity was observed in nematodes that were fed *Achromobacter xylosoxidans* and  
96 *Arcobacter butzleri*, as well as *Citrobacter*, *Escherichia*, *Klebsiella*, *Pseudomonas*, and  
97 *Ralstonia* spp. (Figure 2). A detailed list of all bacterial strains and their effect on polyQ  
98 aggregation is summarized in Table S1. Intriguingly, our data align with previous research  
99 linking the depletion or enrichment of these bacteria in patients with PCDs, which is further  
100 described in the discussion section of the present study. To our knowledge, this is the first-ever  
101 comprehensive screen that assessed the effect of human bacterial isolates on host proteostasis.

102  
103 [Place **Figure 2** here]

104  
105 ***Prevotella* spp. mitigate the proteotoxic aggregation of diverse culprit proteins**  
106 Out of the 229 strains tested, the *Prevotella* genus had the highest number of members that  
107 suppressed polyQ aggregation. We further retested 17 *Prevotella* spp. using the intestinal  
108 polyQ44 model. To increase the robustness of the response, we started feeding animals test  
109 bacteria immediately after hatching. Although we observed an enhanced suppression of  
110 aggregation for most retested strains, there were few isolates that did not significantly inhibit  
111 polyQ aggregation, likely due to the timing of feeding. Furthermore, as expected, feeding worms  
112 test bacteria beginning at the L1 larval stage affected development (Figure 3A, “Aggregates”).  
113 Out of all strains, *P. buccae*, *P. oris*, and *P. corporis* significantly suppressed polyQ aggregation  
114 without causing any detectable developmental delay (Figure 3A, “Aggregates”). Therefore, we  
115 followed up with these three strains. Motility defects are associated with neurodegenerative  
116 PCDs. As such, we assessed whether the three *Prevotella* spp. alleviate aggregate-dependent  
117 motility defects caused by culprit proteins expressed in the intestine and distal tissues. We used  
118 our well-established and validated time-off-pick (TOP) assay that relies on *C. elegans* motility as  
119 a readout of proteotoxicity.<sup>16,17</sup> Consistent with their suppression of polyQ aggregation, all three  
120 strains alleviated aggregate-dependent motility defects with *P. corporis* having the strongest  
121 effect (Figure 3A, “Motility”). To determine whether the observed suppression is dependent on  
122 polyQ, we used N2 wild-type worms and a model expressing a shorter polyglutamine tract,  
123 polyQ33. The results revealed no effect on the N2 worms and a less robust suppression of the  
124 motility defect for polyQ33, indicating that *Prevotella* suppressed proteotoxicity.

125  
126 [Place **Figure 3** here]

127  
128 To determine whether *Prevotella* also affects polyQ in distal tissues, we employed the neuronal  
129 and muscle models. Because worms expressing the neuronal polyQ do not exhibit quantifiable  
130 aggregates, we used the TOP assay as a motility readout. Our results show that of the three  
131 strains, only *P. corporis* showed significant suppression of the motility defect in worms  
132 expressing neuronal polyQ40 (Figure 3B). Unexpectedly, *P. buccae*, *P. oris*, and *P. corporis*  
133 increased motility defects in the neuronal empty vector control (polyQ0); the reason for this is  
134 unknown, but importantly does not diminish the observed beneficial effects of *Prevotella* on  
135 neuronal polyQ. In a manner similar to the intestinal polyQ, we observed *Prevotella*-mediated  
136 suppression of aggregation and proteotoxicity in worms expressing muscle-specific polyQ  
137 (Figure 3C).

138

139 The association between the low abundance of gut *Prevotella* and diverse neurodegenerative  
140 PCDs suggests that the bacterial influence on these diseases is independent of the culprit protein  
141 species.<sup>8-14</sup> As such, we hypothesized that bacteria might affect protein aggregation by  
142 modulating host proteostasis, and if this is the case, *Prevotella* spp. should enhance proteostasis  
143 in worms expressing various aggregation-prone proteins. To test the effect of *Prevotella* on other  
144 disease-associated proteins, we chose three muscle-specific models: one expressing A $\beta$ <sub>1-42</sub>, and  
145 two expressing  $\alpha$ -synuclein.<sup>18-20</sup> These culprit proteins model Alzheimer's and Parkinson's  
146 diseases, respectively. Additionally, these models exhibit age-dependent proteotoxicity, which is  
147 consistent with the age-dependent progression of neurodegenerative diseases.<sup>16,21,22</sup> To  
148 investigate progressive proteotoxicity in the A $\beta$ <sub>1-42</sub> and  $\alpha$ -synuclein models,<sup>18-20</sup> we assessed  
149 their motility between days three to five post-hatching (Figure S2). Nematodes expressing A $\beta$ <sub>1-42</sub>  
150 and  $\alpha$ -synuclein had age-dependent motility defects that were markedly greater than those of the  
151 controls (Figure S2). We examined the effect of *P. buccae*, *P. oris*, and *P. corporis* on  
152 proteotoxicity associated with each of these three models. In a manner similar to the polyQ  
153 models, *P. buccae*, *P. oris*, and *P. corporis* reduced aggregate-dependent toxicity compared to  
154 wild-type control (Figure 3A), particularly with *P. corporis* having the strongest effect (Figure  
155 3D, Figure 3E). Bacteria that strongly enhance or suppress host proteostasis induce notable  
156 differences in the aggregation of A $\beta$ <sub>1-42</sub>, which parallels the extent of the motility defect (Figure  
157 S1). Both A $\beta$ <sub>1-42</sub> aggregation and the associated toxicity were suppressed by *P. corporis* and  
158 enhanced by *Pseudomonas aeruginosa* (Figure S1), a bacterium that strongly disrupted host  
159 proteostasis in our previous studies.<sup>16,23</sup> All of our transgenic worms express exogenous proteins.  
160 To determine whether *Prevotella* can also provide protection against misfolding of endogenous  
161 proteins, we used a strain that carries a temperature-sensitive mutation in myosin heavy chain  
162 (UNC-54) that leads to its misfolding and paralysis at the restrictive temperature (25°C).<sup>24,25</sup> In  
163 agreement with the proteoprotective effect against misfolding and aggregation of exogenous  
164 proteins, *Prevotella* suppressed the temperature-dependent motility defect at the restrictive  
165 temperature, further supporting its beneficial role (Figure S3). Collectively, our findings suggest  
166 the broader potential of *Prevotella* in mitigating the pathogenesis of neurodegenerative diseases.

167

### 168 **Proteotoxic bacteria enhance the aggregation and toxicity of PCD-associated proteins**

169 To confirm the effect of the most robust proteotoxic strains identified in our original screen  
170 (Figure 2, Table S1), we assessed polyQ44 aggregation in animals fed gram-negative aerobes  
171 (Figure 4A, "Aggregates"). We concentrated on these specific bacteria because they did not  
172 affect worm development, which is known to influence proteostasis.<sup>26</sup> We found that *Ralstonia*  
173 sp., *Achromobacter xylosoxidans*, *Pseudomonas* sp., and *K. pneumoniae* were the strongest  
174 inducers of polyQ aggregation (Figure 4A). As we have already demonstrated the proteotoxic  
175 potential of *P. aeruginosa* in our previous work,<sup>16,23</sup> we focused on the three remaining species  
176 in follow-up experiments. To assess the proteotoxic effect of these bacteria, we employed the  
177 TOP assay to measure the motility of worms expressing aggregating polyQ44 and non-  
178 aggregating polyQ33. While we detected a significant enhancement in the motility defect in  
179 animals expressing polyQ44, no significant changes were observed in wild-type or in animals  
180 expressing polyQ33 (Figure 4A). These results indicate that the impairment of motility induced  
181 by bacteria is contingent on polyQ aggregation rather than general bacterial pathogenicity. The  
182 aggregate-dependent motility defects were also observed in worms expressing neuronal and  
183 muscle-specific polyQ; although, the phenotype was less robust as we did detect some decrease  
184 in motility in control animals (Figures 4B and 4C). *K. pneumoniae*, *Ralstonia* sp., and *A.*

185 *xylosoxidans* also elevated muscle-specific polyQ aggregation (Figure 4C). To test the microbial  
186 influence on other disease-associated proteins, we employed worms expressing muscle-specific  
187 A $\beta$ <sub>1-42</sub> and  $\alpha$ -synuclein. In agreement with the intestinal polyQ model, all of these bacterial  
188 isolates also induced proteotoxicity associated with these additional culprit proteins (Figures 4D  
189 and E). These results demonstrate that bacteria can enhance the proteotoxicity of diverse disease-  
190 associated proteins, supporting their role in the pathogenesis of neurodegenerative PCDs.

191

192 [Place **Figure 4** here]

193

## 194 **Discussion**

195 In the present study, we screened a comprehensive collection of 229 unique bacterial isolates  
196 from the Human Microbiome Project for their ability to affect host proteostasis from within the  
197 intestinal milieu. Our follow-up experiments on the most robust beneficial and detrimental  
198 bacteria confirmed their influence on proteostasis across host tissues, affecting the stability of  
199 proteins associated with Alzheimer's, Parkinson's, and Huntington's diseases. The phylogenetic  
200 analysis revealed clustering of select proteotoxic and proteoprotective bacteria, indicating that  
201 genetically related bacteria affect host proteostasis in a similar manner, but with a different  
202 magnitude (Figure S4). To our knowledge, this is the first comprehensive characterization of  
203 bacteria from human microbiomes on host proteostasis. Surprisingly, our data suggest that  
204 bacteria do not selectively target any specific host proteins associated with PCDs, but rather  
205 affect proteostasis in general, leading to the aggregation and proteotoxicity of any destabilized  
206 proteins present within the proteome, such as exogenous polyQ, A $\beta$ <sub>1-42</sub>, and  $\alpha$ -synuclein, tested  
207 in our experiments. While this is a generalized mechanism, there could be microbes that  
208 exclusively affect a specific disease.

209

210 Numerous studies that employed genomic analyses of microbial compositions in affected  
211 patients revealed a connection between comparable gut dysbioses and diverse neurodegenerative  
212 PCDs.<sup>6</sup> These correlational studies from human subjects support our conclusion that bacteria  
213 impact protein stability by modulating host proteostasis. This mechanism is likely mediated by  
214 the interplay between host proteostasis and immune responses to bacteria.<sup>27,28</sup>

215

216 Many of the studies aiming to identify neurodegenerative PCD etiology or treat the disease have  
217 centered on host-targeted therapeutics, primarily focused on targeting the aggregating proteins or  
218 the affected cell types. However, this approach has not been successful in pre-clinical or clinical  
219 trials.<sup>29,30</sup> Perhaps the focal point of the host-targeted approach occurs too late in the aggregation  
220 cascade given that the changes in the gut microbiota can happen prior to any clinical  
221 manifestation.<sup>31,32</sup> Indeed, individuals with neurodegenerative PCDs have insufficient  
222 proteostatic capacity.<sup>33</sup> While some studies have attempted to treat neurodegenerative PCDs by  
223 enhancing components of the host proteostasis network, these have not been successful.<sup>29</sup> In  
224 support of our results indicating that bacteria affect host proteostasis, a shift towards microbial-  
225 centered therapeutic approaches has shown more promise in lessening disease symptoms. For  
226 example, eradication of *H. pylori* in AD patients was associated with improved disease  
227 presentation in a clinical trial and a population-based study.<sup>34,35</sup> Interestingly, the beneficial  
228 effect of antibiotics on the progression of PCDs, when administered post-onset, is absent when  
229 antibiotics were used prior to disease onset; notably, general antibiotic use has been associated  
230 with increased risk for PCDs as well as gut dysbiosis.<sup>36-38</sup> While *H. pylori* is a good clinical

231 example of microbial contribution to neurodegenerative diseases, we did not expect to detect  
232 proteotoxicity associated with this bacterium in our *C. elegans* model due to a limitation of our  
233 approach that includes transferring and incubating bacteria at sub-optimal temperature – a factor  
234 that facilitates *H. pylori* virulence.<sup>39</sup> Additional reports suggest that *H. pylori* can indirectly  
235 affect the composition of the human gut microbiota.<sup>40</sup> Microbe-targeted therapeutic approaches  
236 hold promise and are further bolstered by a recent study that demonstrated that gut microbiota  
237 and serum derived from AD patients accelerate disease symptoms and affect neurogenesis in  
238 healthy rats and tissue culture, respectively.<sup>41</sup>

239  
240 In our screen (Figure 2), *Prevotella* stood out as the only genus devoid of any species that exhibit  
241 proteotoxicity towards the host. Furthermore, our findings indicate that *Prevotella* spp. have a  
242 broad and suppressive effect on host protein aggregation, regardless of the specific disease-  
243 associated protein (Figure 3). Sequencing data suggest that a low abundance of *Prevotella* in the  
244 guts of patients with PCDs enhances disease pathogenesis.<sup>7-14</sup> However, despite the fact that the  
245 *Prevotella* genus contains over 50 species, many studies report their results at the genus level.<sup>42</sup>  
246 Our data indicate that various *Prevotella* species exhibit a differential effect on host proteostasis  
247 (Figure 3A). Such various effects of individual species could be explained by large variability in  
248 their genomes.<sup>42</sup> The species, *P. intermedia*, *P. nigrescence*, and *P. melanigencia* have been  
249 consistently associated with infection,<sup>43-45</sup> inflammation,<sup>46-49</sup> and have also been linked to AD  
250 and associated mortality.<sup>50</sup> Conversely, it has been shown that *P. buccae* and *P. corporis*, two  
251 strains of *Prevotella* that exhibited strong suppression of protein aggregation and the associated  
252 toxicity, were found not to induce inflammation.<sup>51</sup> Instead, *P. buccae* and *P. corporis* were  
253 shown to induce the expression of mucin-associated membrane proteins MUC3 and MUC4.<sup>51</sup>  
254 Interestingly, induction of MUC3 expression by a probiotic cocktail prevented adherence of  
255 enteropathogenic *E. coli*.<sup>52</sup> MUC4 has been shown to be essential for maintaining mucus barrier  
256 function and intestinal homeostasis in mice, as its absence resulted in severe large intestinal  
257 bleeding and significant down regulation of antimicrobial peptides.<sup>53</sup> Though preliminary, the  
258 evidence suggesting the protective role of *Prevotella* in maintaining intestinal integrity is  
259 interesting, as intestinal integrity is often compromised in people with neurodegenerative  
260 PCDs.<sup>54</sup> Damage to the intestinal epithelium can lead to translocation of bacteria and bacterial  
261 products, resulting in systemic inflammation and the breakdown of the blood-brain barrier,  
262 contributing to a variety of diseases, including PCDs.<sup>55,56</sup> The contrasting associations of  
263 different *Prevotella* species in host health and disease, highlight the importance of studying  
264 bacteria at the species level, as demonstrated in the present study, to unravel the precise roles of  
265 bacteria in disease pathogenesis.

266  
267 The physiological relevance of our findings is supported by studies that focus on pathogenic  
268 bacteria and subsequently establish a connection with PCDs. For example, the robust induction  
269 of proteotoxicity by *K. pneumoniae* across all *C. elegans* models expressing different  
270 aggregation-prone protein species (Figure 4), is in agreement with a previous study that  
271 identified an overabundance of *K. pneumoniae* in the gut microbiota of individuals with AD.<sup>57</sup>  
272 Furthermore, a positive correlation has been demonstrated between the presence of *K.*  
273 *pneumoniae* in the gut and elevated levels of the AD biomarker, C-reactive protein, in blood  
274 samples of AD patients.<sup>58</sup> Another study found an elevated abundance of *Ralstonia* in mucosal  
275 samples from individuals with PD,<sup>59</sup> which is another bacterium that was robustly proteotoxic to  
276 our *C. elegans* models (Figure 4). Interestingly, this bacterium was also found to be more

277 prevalent in individuals with autism,<sup>60</sup> which is another disease that has been associated with the  
278 presence of misfolded proteins.<sup>61-64</sup> Autism has also been associated with both *Achromobacter*  
279 and *Pseudomonas* genera.<sup>65,66</sup> Both *Achromobacter* and *Pseudomonas* are linked to cystic  
280 fibrosis, which is another PCD that does not feature neurodegeneration;<sup>67,68</sup> *Achromobacter* was  
281 reported to exacerbate the disease,<sup>69</sup> and *P. aeruginosa* is a predominant pathogenic species that  
282 colonizes the lungs of CF patients.<sup>70</sup> *A. xylosoxidans* induced proteotoxicity in all our disease  
283 models (Figure 4), along with *Pseudomonas*, which displayed a notable increase in polyQ  
284 aggregation (Figure 4A, "Aggregates"). Furthermore, we previously demonstrated that *P.*  
285 *aeruginosa* exert robust proteotoxic effects on *C. elegans*.<sup>16,23</sup> The presence of *Pseudomonas*, in  
286 conjunction with another bacterial genus, was successfully used to differentiate individuals with  
287 AD from control subjects.<sup>71</sup> Collectively, the aforementioned studies are in agreement with our  
288 results and further support the wide-ranging impact of bacteria on protein folding diseases. It is  
289 remarkable that the abovementioned bacteria induce proteotoxicity consistently across all our *C.*  
290 *elegans* models expressing distinct disease proteins. The convergence of our results with existing  
291 literature linking these bacteria to PCDs strongly reinforces the notion that bacteria affect the  
292 host proteostasis network, broadly affecting protein stability.

293  
294 While our results support a wider-reaching impact of bacteria on the stability of host proteins, it  
295 is worth noting that bacteria can selectively target components of the host proteostasis network.  
296 For example, *P. aeruginosa* produces toxins that target the mitochondrial unfolded protein  
297 response (UPR<sup>MT</sup>),<sup>72</sup> a transcriptional pathway that ensures proper protein folding and  
298 clearance.<sup>73</sup> As such, when the UPR<sup>MT</sup> is overwhelmed or disrupted, proteotoxicity can occur,  
299 leading to accelerated protein aggregation.<sup>74</sup> Our previous work demonstrated that *P. aeruginosa*  
300 and *E. coli* can also disrupt host proteostasis through the production of bacteria-derived protein  
301 aggregates.<sup>16,23</sup> Additionally, *P. aeruginosa* FapC amyloids were shown to cross-seed with A $\beta$ <sub>1-42</sub>.<sup>75</sup>  
302 Interestingly, the *fap* operon is also present in the genomes of Burkholderiales, which  
303 include *Ralstonia* and *Achromobacter*.<sup>76,77</sup> The *E. coli* amyloid, curli, enhanced the aggregation  
304 of  $\alpha$ -synuclein *in vivo*.<sup>78</sup> *K. pneumoniae* is also capable of producing amyloids,<sup>79</sup> and was  
305 proteotoxic to all *C. elegans* lines (Figure 4). The underlying mechanisms of the bacteria-  
306 induced proteotoxicity remain elusive; however, it is likely that metastable proteins of bacterial  
307 origin sequester host chaperones. Such sequestration would diminish the capacity of the  
308 proteostasis network to buffer folding of endogenous proteins. A similar mechanism is supported  
309 by the organismal ability to buffer protein polymorphisms present within the host proteome,  
310 which is hindered by the introduction of misfolded proteins.<sup>80</sup>

311  
312 A comprehensive understanding of individual bacterial residents of the human microbiota in the  
313 pathogenesis of neurodegenerative PCDs is crucial in developing effective interventions. Our  
314 study challenges the traditional approach of solely focusing on host-targeted therapeutics for  
315 neurodegenerative PCDs. Instead, modulating the gut microbiota may offer an effective strategy  
316 for preventing and managing these devastating diseases. Gut-targeted interventions will likely  
317 have to be implemented early in the disease or even prior to its onset. While our results indicate  
318 that bacteria generally affect host proteostasis, ultimately influencing the stability of host  
319 proteins, further studies are needed to decipher the role of proteoprotective and proteotoxic  
320 species in humans and devise approaches to control their levels.

## 321 Acknowledgments

323 We thank Dr. Richard Morimoto and Sue Fox for providing *C. elegans* polyQ strains  
324 (Northwestern University), and Dr. Janine Kirstein (Leibniz Institute on Aging– Fritz Lipmann  
325 Institute) for providing *C. elegans* A $\beta$ <sub>1-42</sub> strain and the control. The other *C. elegans* strains were  
326 provided by the Caenorhabditis Genetics Center, which is funded by the NIH Office of Research  
327 Infrastructure Programs (P40 OD010440). Human bacterial isolates (listed in Table S1) were  
328 obtained through BEI Resources, NIAID, and NIH as part of the Human Microbiome Project.  
329 We thank Mark Gorelik for training RB and for assistance with computational analysis. We  
330 would like to thank the funders who have supported our work on the bacterial contribution to  
331 protein conformational diseases, namely the National Institute on Aging (R03AG070580), and  
332 the Infectious Diseases Society of America. Furthermore, we would like to thank the Department  
333 of Microbiology and Cell Science for start-up funding. Figure 1 was created using  
334 BioRender.com.

### 335 **Author contributions**

336 DMC: conceived the project. ACW and DMC designed the study, analyzed data, and wrote the  
337 manuscript. ACW, RB, ASB performed the experiments. ACW and MB data visualization.

### 338 **Declaration of interests**

339 The authors declare no competing interest.

### 340 **Legends**

341 **Figure 1. Schematic illustrating the method used to assess the effect of bacterial isolates on**  
342 ***C. elegans* proteostasis.** Details can be found in Star Methods.

343 **Figure 2. Heat map showing the extent of the screen that identified the effect of human**  
344 **bacterial isolates on *C. elegans* intestinal polyQ aggregation.** Aggregation data are normalized  
345 to worms fed control *E. coli* OP50.

346 **Figure 3. The effect of *Prevotella* spp. on proteins associated with neurodegenerative**  
347 **diseases.** A) The effect of *Prevotella* spp. on *C. elegans* intestinal polyQ aggregation  
348 ("Aggregates") and the associated toxicity ("Motility"). Checkered bars represent bacteria-  
349 associated developmental delay. The three strongest suppressors of polyQ aggregation that did  
350 not affect development were tested using intestinal polyQ, B) neuronal polyQ, C) muscle polyQ,  
351 D) muscle A $\beta$ <sub>1-42</sub>, and E) muscle  $\alpha$ -synuclein. Data are represented as the average number of  
352 aggregates or TOP (seconds) per worm obtained from at least two independent experiments for a  
353 total of 30-60 worms. Error bars represent standard error of the mean (SEM). Statistical  
354 significance was calculated using one-way ANOVA followed by multiple comparison Dunnett's  
355 post-hoc test (\*p<0.05, \*\*p<0.01, \*\*\*p<0.001, \*\*\*\*p<0.0001).

356 **Figure 4. The effect of proteotoxic bacteria on proteins associated with neurodegenerative**  
357 **diseases.** A) The effect of gram-negative, aerobic bacteria on *C. elegans* intestinal polyQ  
358 aggregation ("Aggregates") and the associated toxicity ("Motility"). Three robust enhancers of  
359 polyQ aggregation were tested using intestinal polyQ, B) neuronal polyQ, C) muscle polyQ, D)  
360 muscle A $\beta$ <sub>1-42</sub>, and E) muscle  $\alpha$ -synuclein. Data are represented as the average number of  
361 aggregates or TOP (seconds) per worm obtained from at least two independent experiments for a  
362 total of 30-60 worms. Error bars represent SEM. Statistical significance was calculated using



369 one-way ANOVA followed by multiple comparison Dunnett's post-hoc test (\* $p < 0.05$ , \*\* $p < 0.01$ ,  
370 \*\*\* $p < 0.001$ , \*\*\*\* $p < 0.0001$ ).

371

372

## 373 **STAR Methods**

374

### 375 **Key resources table**

376 *C. elegans* and bacterial strains that are not from the BEI repository can be found in Table 1.

377

### 378 ***C. elegans* maintenance and strains**

379 *C. elegans* were maintained as previously described.<sup>16</sup> For experiments that generated the data  
380 represented in the heat-map (Figure 2), nematodes were kept on *E. coli* OP50 for two days at  
381 20°C, washed three times and transferred to indicated bacteria, where they were kept at 22.5°C  
382 for three days. For all other experiments, nematodes were plated on indicated bacteria as L1s at  
383 22.5°C, where they remained until the time of assay, except for the experiment in Figure S3, in  
384 which worms were cultured in temperatures indicated in the figure. All *C. elegans* strains used in  
385 this study can be found in Table 1.

386

### 387 **Bacterial culture conditions**

388 All bacteria were cultured at 37°C. Parenthesized numbers (1-5) in ST1 reflect the remaining  
389 conditions in which bacteria were grown in the heat-map (Figure 2): 1) anaerobically in  
390 reinforced clostridial broth (RCB) with Oxyrase, 2) facultative conditions (no shaking, tube filled  
391 to top) in brain heart infusion broth (BHI), 3) aerobic conditions, shaking at 220 revolutions per  
392 minute (RPM) in BHI, 4) anaerobic conditions on tryptic soy agar (TSA) supplemented with 5%  
393 defibrinated sheep's blood, 5) aerobic conditions on TSA supplemented with 5% defibrinated  
394 sheep's blood. *E. coli* OP50 controls were grown in a manner consistent with which experiment  
395 was performed. Bacteria were washed and resuspended in M9 before being seeded on NGM. All  
396 follow-up experiments were performed with bacteria grown on TSA supplemented with 5%  
397 defibrinated sheep's blood at 37°C except for the intestinal confirmation experiment of the  
398 proteotoxic bacteria (Figure 4A, "Aggregates"). Except for *Prevotella* spp. which were grown  
399 under anaerobic conditions, bacteria were grown aerobically in follow-up experiments.

400

### 401 **Aggregate quantification**

402 Fluorescent aggregates were quantified using Leica MZ10F Modular Stereo Microscope  
403 equipped with CoolLED pE300lite 365 dir mount STEREO with filter set ET GFP-MZ10F.  
404 Fluorescent aggregates in worms used to generate data for the heat-map (Figure 2, Table S1)  
405 were manually quantified after having been cultured as indicated in "*C. elegans* maintenance and  
406 strains". For all other experiments, worms were plated on indicated bacteria as L1s and  
407 fluorescent aggregates were manually quantified after four days (intestinal polyQ44) or three  
408 days (muscle polyQ35, 40) of life as previously described.

409

### 410 **Motility assays**

411 All motility assays were performed at room temperature as previously described.<sup>16</sup> Time-off-pick  
412 (seconds) of transgenic nematodes harboring tissue-specific aggregating protein species was  
413 assessed as previously described,<sup>16,17</sup> on three days (muscle polyQ, muscle A $\beta$ <sub>1-42</sub>, T $\Delta$  and

414 respective controls) or four days (intestine polyQ, neuron polyQ, muscle  $\alpha$ -synuclein and  
415 control) after having been plated on indicated bacteria as L1s.

416

### 417 **Live imaging**

418 Nematodes expressing muscle-specific A $\beta$ <sub>1-42</sub> were plated as L1s on NGM containing *E. coli*  
419 OP50, *P. corporis* HM-1294, and *P. aeruginosa* PAO1 for three days were mounted, frozen to  
420 reduce background fluorescence, and imaged. Fluorescent and Nomarski images were taken  
421 using Zeiss Axio Observer 7, equipped as described previously.<sup>16</sup> Images were processed as  
422 previously described.<sup>16</sup>

423

### 424 **Gel electrophoresis and western blotting**

425 Worms were prepared for gel electrophoresis and western blotting which were performed as  
426 previously described with a few modifications.<sup>16</sup> In brief, M9 was used to lift worms from NGM  
427 which were washed until superficial bacteria was removed. Worms were plated on unseeded  
428 NGM, were allowed to dry briefly and 50 worms were picked into 10  $\mu$ L M9 with 1mM  
429 phenylmethylsulfonyl fluoride (PMSF) in non-skirted screw-cap microcentrifuge tubes and  
430 frozen overnight or longer at -80°C. Tubes were pulse-centrifuged and three, 1.5mm zirconium  
431 beads were added to each tube. The following two steps were repeated a minimum of two times;  
432 if large worm particulates were observed, these steps were repeated again with the entire sample  
433 set until no tubes contained worm pieces that were visible under a dissecting microscope:  
434 Samples were homogenized by placing tubes in a Bead Bug homogenizer at 280x10 rates per  
435 minute (RPM) for 90 seconds. Tubes were cooled on ice and centrifuged for 1-2 minutes on a  
436 low speed to re-settle worms and worm particulates. Samples were prepped for gel  
437 electrophoresis as previously described,<sup>16</sup> and entire samples were loaded on 4-12% gradient  
438 sodium dodecylsulfate-polyacrylamide gels (SDS-PAGE) to separate proteins through  
439 electrophoresis. Proteins were transferred onto polyvinyl difluoride (PDVF) membrane, blocked  
440 with 5% nonfat milk powder in PBS-Tween-20 (PBST) and probed with Living Colors JL-8  
441 monoclonal primary antibody (1:1000) for 48 hours at 4C on orbital shaker and underwent three,  
442 five-minute washes with 0.1% PBST followed by incubation 1:10,000 with goat-anti-mouse  
443 horse-radish peroxidase (HRP) conjugated secondary antibody for at least two hours followed by  
444 three, ten-minute washes with 0.1% PBST. Chemiluminescence was achieved by incubation with  
445 Clarity Western ECL substrate. Image J (v1.52) was used to analyze insoluble fractions.

446

### 447 **Quantification and statistical analysis**

448 Quantification of aggregate counts per worm in Figure 2 were performed on a cohort of ten  
449 worms to corroborate the findings from the western blot analysis. In the rest of the figures, data  
450 are represented as the average number of aggregates or TOP (seconds) per worm obtained from  
451 two independent experiments for a total of 45-60 worms (Figure 3A "Aggregates"), 60 worms  
452 (Figure 4A "Aggregates"); three independent experiments for a total of 45 worms (Figure 3A  
453 "Motility", Figure 3B, Figure 3C, Figure 4A "Motility", Figure 4C "Aggregates") or 30 worms  
454 (Figure 3D, Figure 3E, Figure 4B, Figure 4C "Motility", Figure 4D, Figure 4E, Figure S1B,  
455 Figure S3); two independent experiments for a total of 20 worms (Figure S2). Data are described  
456 as statistically significant when  $p < 0.05$  as determined by Student's t-test or one-way ANOVA  
457 followed by multiple comparison Dunnett's post-hoc test performed using Graphpad Prism 8.4.3  
458 or later. Degrees of significance are denoted by the use of asterisks such that \* $p < 0.05$ , \*\* $p < 0.01$ ,

459 \*\*\* $p < 0.001$ , \*\*\*\* $p < 0.0001$ . The heat map (Figure 1) is represented as data normalized to the  
460 control *E. coli* OP50. Error bars represent standard error of the mean.

461

### 462 **Heat map generation**

463 Heatmap was constructed in R-studio using the ComplexHeatmap package from the  
464 Bioconductor project. The experimental data were fed into R-studio as an organized .CSV file.  
465 The heatmap is the graphical representation of this data, clustering the bacteria by phylum.

466

### 467 **Phylogenetic tree generation**

468 Whole genome sequences were assembled using the Bacterial and Viral Bioinformatics  
469 Resources Center (BV-BCR) via Unicycler. All genomes were annotated in BV-BRC using  
470 Prokka. Phylogenetic analysis was conducted in BV-BRC based on concatenated alignments of  
471 100 single-copy genes using mafft, and the results were assessed for maximum likelihood using  
472 RAxML. Sequences that did not have 100 complete single-copy genes due to poor sequencing  
473 quality were excluded.

474

## 475 SUPPLEMENTAL INFORMATION TITLES AND LEGENDS

476 **Fig. S1. The robust effect of bacteria on the aggregation of  $A\beta_{1-42}$  correlates with aggregate-**  
477 **dependent changes in motility.** (A) Nomarski and fluorescent images (mScarlet) and the  
478 corresponding (B) TOP motility measurements of transgenic worms expressing muscle-specific  
479  $A\beta_{1-42}$  fed a proteoprotective strain (*P. corporis*) and a proteotoxigenic strain (*P. aeruginosa*). Each  
480 TOP data point is representative of the average of three independent experiments for a total of 30  
481 worms. Error bars represent SEM. Statistical significance was calculated using one-way analysis  
482 of variants (ANOVA) followed by multiple comparison Dunnett's post-hoc test (\* $p < 0.05$ ,  
483 \*\* $p < 0.01$ , \*\*\* $p < 0.001$ ). Scale bar is 100  $\mu\text{m}$ .

484

485 **Fig. S2. Aggregate-dependent toxicity in transgenic animals harboring  $A\beta_{1-42}$  and  $\alpha$ -**  
486 **synuclein is age-dependent.** Age-dependent changes in the motility of animals expressing  
487 muscle-specific (A)  $A\beta_{1-42}$  and (B)  $\alpha$ -synuclein and corresponding control animals: empty vector  
488 (No  $A\beta$ ) and wild-type N2 (WT). Data are represented as the average TOP (seconds) per worm.  
489 Each data point is representative of two independent experiments for a total of 20 worms. Error  
490 bars represent SEM. Statistical significance was calculated using one-way analysis of variants  
491 (ANOVA) followed by multiple comparison Dunnett's post-hoc test (\*\*\* $p < 0.001$ ,  
492 \*\*\*\* $p < 0.0001$ ).

493

494 **Figure S3. *P. corporis* prevents temperature-dependent motility defect.** Temperature-  
495 dependent changes in the motility of animals expressing a muscle-specific mutation in the  
496 myosin heavy-chain gene (*e1301*). Data are represented as the average TOP (seconds) per worm.  
497 Each data point is representative of three independent experiments for a total of 30 worms. Error  
498 bars represent SEM. Statistical significance was calculated using one-way analysis of variants  
499 (ANOVA) followed by multiple comparison Dunnett's post-hoc test (\*\*\*\* $p < 0.0001$ ).

500

501 **Figure S4. Phylogenetic grouping reflects the effect of bacteria on host proteostasis.**

502 Phylogenetic tree shows that proteotoxigenic bacteria predominantly cluster together, separate from  
503 proteoprotective bacteria which also form their own distinct cluster. The size of the bacterial  
504 identifiers is proportional to the magnitude of their respective proteotoxigenic or proteoprotective

505 effects. Proteoprotective bacteria are indicated in blue, and proteotoxic bacteria in red. Tree  
506 analysis was performed on a large collection of human microbiome isolates in BV-BRC using  
507 maximum likelihood based on concatenated alignments of 100 single-copy genes.

508  
509 **Table S1. Data used to generate Figure 2.** "Western" indicates the band intensity of the polyQ  
510 insoluble fraction of worms fed indicated bacteria normalized to those fed *E. coli* OP50 control.  
511 "Count" indicates the average number of aggregates per worm of worms fed indicated bacteria  
512 normalized to those fed *E. coli* OP50 control. Parenthesized numbers (1-5) reflect the remaining  
513 conditions in which bacteria were grown: 1) anaerobically in reinforced clostridial broth (RCB)  
514 with Oxyrase, 2) facultative conditions (no shaking, tube filled to top) in brain heart infusion  
515 broth (BHI), 3) aerobic conditions, shaking at 220 revolutions per minute (RPM) in BHI, 4)  
516 anaerobic conditions on tryptic soy agar (TSA) supplemented with 5% defibrinated sheep's  
517 blood, 5) aerobic conditions on TSA supplemented with 5% defibrinated sheep's blood.

## 518 519 **References**

- 520 (1) Soto, C. Unfolding the Role of Protein Misfolding in Neurodegenerative Diseases. *Nat. Rev.*  
521 *Neurosci.* **2003**, *4* (1), 49–60. <https://doi.org/10.1038/nrn1007>.
- 522 (2) 2022 Alzheimer's Disease Facts and Figures. *Alzheimers Dement. J. Alzheimers Assoc.* **2022**,  
523 *18* (4), 700–789. <https://doi.org/10.1002/alz.12638>.
- 524 (3) Oliphant, K.; Allen-Vercoe, E. Macronutrient Metabolism by the Human Gut Microbiome:  
525 Major Fermentation by-Products and Their Impact on Host Health. *Microbiome* **2019**, *7* (1),  
526 91. <https://doi.org/10.1186/s40168-019-0704-8>.
- 527 (4) Clarke, G.; Stilling, R. M.; Kennedy, P. J.; Stanton, C.; Cryan, J. F.; Dinan, T. G.  
528 Minireview: Gut Microbiota: The Neglected Endocrine Organ. *Mol. Endocrinol.* **2014**, *28*  
529 (8), 1221–1238. <https://doi.org/10.1210/me.2014-1108>.
- 530 (5) Intili, G.; Paladino, L.; Rappa, F.; Alberti, G.; Plicato, A.; Calabrò, F.; Fucarino, A.;  
531 Cappello, F.; Bucchieri, F.; Tomasello, G.; Carini, F.; Pitruzzella, A. From Dysbiosis to  
532 Neurodegenerative Diseases through Different Communication Pathways: An Overview.  
533 *Biology* **2023**, *12* (2), 195. <https://doi.org/10.3390/biology12020195>.
- 534 (6) Fang, P.; Kazmi, S. A.; Jameson, K. G.; Hsiao, E. Y. The Microbiome as a Modifier of  
535 Neurodegenerative Disease Risk. *Cell Host Microbe* **2020**, *28* (2), 201–222.  
536 <https://doi.org/10.1016/j.chom.2020.06.008>.
- 537 (7) Jin, M.; Li, J.; Liu, F.; Lyu, N.; Wang, K.; Wang, L.; Liang, S.; Tao, H.; Zhu, B.; Alkasir, R.  
538 Analysis of the Gut Microflora in Patients With Parkinson's Disease. *Front. Neurosci.*  
539 **2019**, *13*.
- 540 (8) Scheperjans, F.; Aho, V.; Pereira, P. A. B.; Koskinen, K.; Paulin, L.; Pekkonen, E.;  
541 Haapaniemi, E.; Kaakkola, S.; Eerola-Rautio, J.; Pohja, M.; Kinnunen, E.; Murros, K.;  
542 Auvinen, P. Gut Microbiota Are Related to Parkinson's Disease and Clinical Phenotype.  
543 *Mov. Disord. Off. J. Mov. Disord. Soc.* **2015**, *30* (3), 350–358.  
544 <https://doi.org/10.1002/mds.26069>.
- 545 (9) Hertzberg, V. S.; Singh, H.; Fournier, C. N.; Moustafa, A.; Polak, M.; Kuelbs, C. A.;  
546 Torralba, M. G.; Tansey, M. G.; Nelson, K. E.; Glass, J. D. Gut Microbiome Differences  
547 between Amyotrophic Lateral Sclerosis Patients and Spouse Controls. *Amyotroph. Lateral*  
548 *Scler. Front. Degener.* **2022**, *23* (1–2), 91–99.  
549 <https://doi.org/10.1080/21678421.2021.1904994>.

- 550 (10) Vidal-Martinez, G.; Chin, B.; Camarillo, C.; Herrera, G. V.; Yang, B.; Sarosiek, I.; Perez,  
551 R. G. A Pilot Microbiota Study in Parkinson's Disease Patients versus Control Subjects,  
552 and Effects of FTY720 and FTY720-Mitoxo Therapies in Parkinsonian and Multiple  
553 System Atrophy Mouse Models. *J. Park. Dis.* **2020**, *10* (1), 185–192.  
554 <https://doi.org/10.3233/JPD-191693>.
- 555 (11) Unger, M. M.; Spiegel, J.; Dillmann, K.-U.; Grundmann, D.; Philippeit, H.; Bürmann, J.;  
556 Faßbender, K.; Schwierz, A.; Schäfer, K.-H. Short Chain Fatty Acids and Gut Microbiota  
557 Differ between Patients with Parkinson's Disease and Age-Matched Controls.  
558 *Parkinsonism Relat. Disord.* **2016**, *32*, 66–72.  
559 <https://doi.org/10.1016/j.parkreldis.2016.08.019>.
- 560 (12) Li, F.; Wang, P.; Chen, Z.; Sui, X.; Xie, X.; Zhang, J. Alteration of the Fecal Microbiota in  
561 North-Eastern Han Chinese Population with Sporadic Parkinson's Disease. *Neurosci. Lett.*  
562 **2019**, *707*, 134297. <https://doi.org/10.1016/j.neulet.2019.134297>.
- 563 (13) Bedarf, J. R.; Hildebrand, F.; Coelho, L. P.; Sunagawa, S.; Bahram, M.; Goeser, F.; Bork,  
564 P.; Wüllner, U. Functional Implications of Microbial and Viral Gut Metagenome Changes  
565 in Early Stage L-DOPA-Naïve Parkinson's Disease Patients. *Genome Med.* **2017**, *9* (1), 39.  
566 <https://doi.org/10.1186/s13073-017-0428-y>.
- 567 (14) Aho, V. T. E.; Pereira, P. A. B.; Voutilainen, S.; Paulin, L.; Pekkonen, E.; Auvinen, P.;  
568 Scheperjans, F. Gut Microbiota in Parkinson's Disease: Temporal Stability and Relations to  
569 Disease Progression. *EBioMedicine* **2019**, *44*, 691–707.  
570 <https://doi.org/10.1016/j.ebiom.2019.05.064>.
- 571 (15) Wallen, Z. D.; Demirkan, A.; Twa, G.; Cohen, G.; Dean, M. N.; Standaert, D. G.; Sampson,  
572 T. R.; Payami, H. Metagenomics of Parkinson's Disease Implicates the Gut Microbiome in  
573 Multiple Disease Mechanisms. *Nat. Commun.* **2022**, *13* (1), 6958.  
574 <https://doi.org/10.1038/s41467-022-34667-x>.
- 575 (16) Walker, A. C.; Bhargava, R.; Vaziriyani-Sani, A. S.; Pourciau, C.; Donahue, E. T.; Dove, A.  
576 S.; Gebhardt, M. J.; Ellward, G. L.; Romeo, T.; Czyż, D. M. Colonization of the  
577 *Caenorhabditis Elegans* Gut with Human Enteric Bacterial Pathogens Leads to Proteostasis  
578 Disruption That Is Rescued by Butyrate. *PLOS Pathog.* **2021**, *17* (5), e1009510.  
579 <https://doi.org/10.1371/journal.ppat.1009510>.
- 580 (17) Walker, A. C.; Bhargava, R.; Brust, A. S.; Owji, A. A.; Czyż, D. M. Time-off-Pick Assay  
581 to Measure *Caenorhabditis Elegans* Motility. *Bio-Protoc.* **2022**, *12* (12), e4436.  
582 <https://doi.org/10.21769/BioProtoc.4436>.
- 583 (18) Bodhicharla, R.; Nagarajan, A.; Winter, J.; Adenle, A.; Nazir, A.; Brady, D.; Vere, K.;  
584 Richens, J.; O'Shea, P.; Bell, D. R.; de Pomerai, D. Effects of  $\alpha$ -Synuclein Overexpression  
585 in Transgenic *Caenorhabditis Elegans* Strains. *CNS Neurol. Disord. Drug Targets* **2012**, *11*  
586 (8), 965–975. <https://doi.org/10.2174/1871527311211080005>.
- 587 (19) Ham, T. J. van; Thijssen, K. L.; Breitling, R.; Hofstra, R. M. W.; Plasterk, R. H. A.; Nollen,  
588 E. A. A. *C. Elegans* Model Identifies Genetic Modifiers of  $\alpha$ -Synuclein Inclusion  
589 Formation During Aging. *PLOS Genet.* **2008**, *4* (3), e1000027.  
590 <https://doi.org/10.1371/journal.pgen.1000027>.
- 591 (20) Gallrein, C.; Iburg, M.; Michelberger, T.; Koçak, A.; Puchkov, D.; Liu, F.; Ayala Mariscal,  
592 S. M.; Nayak, T.; Kaminski Schierle, G. S.; Kirstein, J. Novel Amyloid-Beta Pathology *C.*  
593 *Elegans* Model Reveals Distinct Neurons as Seeds of Pathogenicity. *Prog. Neurobiol.* **2021**,  
594 *198*, 101907. <https://doi.org/10.1016/j.pneurobio.2020.101907>.

- 595 (21) Morley, J. F.; Brignull, H. R.; Weyers, J. J.; Morimoto, R. I. The Threshold for  
596 Polyglutamine-Expansion Protein Aggregation and Cellular Toxicity Is Dynamic and  
597 Influenced by Aging in *Caenorhabditis Elegans*. *Proc. Natl. Acad. Sci. U. S. A.* **2002**, *99*  
598 (16), 10417–10422. <https://doi.org/10.1073/pnas.152161099>.
- 599 (22) Taylor, R. C.; Dillin, A. Aging as an Event of Proteostasis Collapse. *Cold Spring Harb.*  
600 *Perspect. Biol.* **2011**, *3* (5), a004440. <https://doi.org/10.1101/cshperspect.a004440>.
- 601 (23) Walker, A. C.; Bhargava, R.; Dove, A. S.; Brust, A. S.; Owji, A. A.; Czyż, D. M. Bacteria-  
602 Derived Protein Aggregates Contribute to the Disruption of Host Proteostasis. *Int. J. Mol.*  
603 *Sci.* **2022**, *23* (9), 4807. <https://doi.org/10.3390/ijms23094807>.
- 604 (24) Ben-Zvi, A.; Miller, E. A.; Morimoto, R. I. Collapse of Proteostasis Represents an Early  
605 Molecular Event in *Caenorhabditis Elegans* Aging. *Proc. Natl. Acad. Sci. U. S. A.* **2009**,  
606 *106* (35), 14914–14919. <https://doi.org/10.1073/pnas.0902882106>.
- 607 (25) Macleod, A. R.; Waterston, R. H.; Fishpool, R. M.; Brenner, S. Identification of the  
608 Structural Gene for a Myosin Heavy-Chain in *Caenorhabditis Elegans*. *J. Mol. Biol.* **1977**,  
609 *114* (1), 133–140. [https://doi.org/10.1016/0022-2836\(77\)90287-X](https://doi.org/10.1016/0022-2836(77)90287-X).
- 610 (26) Labbadia, J.; Morimoto, R. I. Proteostasis and Longevity: When Does Aging Really Begin?  
611 *F1000Prime Rep.* **2014**, *6*, 7. <https://doi.org/10.12703/P6-7>.
- 612 (27) Tansey, M. G.; Wallings, R. L.; Houser, M. C.; Herrick, M. K.; Keating, C. E.; Joers, V.  
613 Inflammation and Immune Dysfunction in Parkinson Disease. *Nat. Rev. Immunol.* **2022**, *22*  
614 (11), 657–673. <https://doi.org/10.1038/s41577-022-00684-6>.
- 615 (28) Walker, A.; Czyz, D. M. Oh My Gut! Is the Microbial Origin of Neurodegenerative  
616 Diseases Real? *Infect. Immun.* **2023**, e0043722. <https://doi.org/10.1128/iai.00437-22>.
- 617 (29) Sweeney, P.; Park, H.; Baumann, M.; Dunlop, J.; Frydman, J.; Kopito, R.; McCampbell, A.;  
618 Leblanc, G.; Venkateswaran, A.; Nurmi, A.; Hodgson, R. Protein Misfolding in  
619 Neurodegenerative Diseases: Implications and Strategies. *Transl. Neurodegener.* **2017**, *6*.  
620 <https://doi.org/10.1186/s40035-017-0077-5>.
- 621 (30) Mullane, K.; Williams, M. Preclinical Models of Alzheimer’s Disease: Relevance and  
622 Translational Validity. *Curr. Protoc. Pharmacol.* **2019**, *84* (1), e57.  
623 <https://doi.org/10.1002/cpph.57>.
- 624 (31) Savica, R.; Carlin, J. M.; Grossardt, B. R.; Bower, J. H.; Ahlskog, J. E.; Maraganore, D. M.;  
625 Bharucha, A. E.; Rocca, W. A. Medical Records Documentation of Constipation Preceding  
626 Parkinson Disease. *Neurology* **2009**, *73* (21), 1752–1758.  
627 <https://doi.org/10.1212/WNL.0b013e3181c34af5>.
- 628 (32) Ferreira, A. L.; Choi, J.; Ryou, J.; Newcomer, E. P.; Thompson, R.; Bollinger, R. M.; Hall-  
629 Moore, C.; Ndao, I. M.; Sax, L.; Benzinger, T. L. S.; Stark, S. L.; Holtzman, D. M.; Fagan,  
630 A. M.; Schindler, S. E.; Cruchaga, C.; Butt, O. H.; Morris, J. C.; Tarr, P. I.; Ances, B. M.;  
631 Dantas, G. Gut Microbiome Composition May Be an Indicator of Preclinical Alzheimer’s  
632 Disease. *Sci. Transl. Med.* **2023**, *15* (700), eabo2984.  
633 <https://doi.org/10.1126/scitranslmed.abo2984>.
- 634 (33) Tseng, C.-S.; Chao, Y.-W.; Liu, Y.-H.; Huang, Y.-S.; Chao, H.-W. Dysregulated  
635 Proteostasis Network in Neuronal Diseases. *Front. Cell Dev. Biol.* **2023**, *11*, 1075215.  
636 <https://doi.org/10.3389/fcell.2023.1075215>.
- 637 (34) Chang, Y.-P.; Chiu, G.-F.; Kuo, F.-C.; Lai, C.-L.; Yang, Y.-H.; Hu, H.-M.; Chang, P.-Y.;  
638 Chen, C.-Y.; Wu, D.-C.; Yu, F.-J. *Eradication of Helicobacter pylori Is Associated with the*  
639 *Progression of Dementia: A Population-Based Study*. *Gastroenterology Research and*  
640 *Practice*. <https://doi.org/10.1155/2013/175729>.

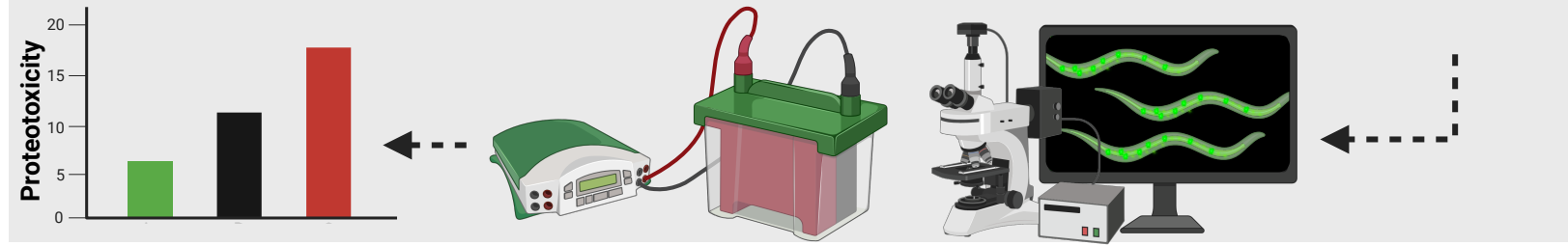
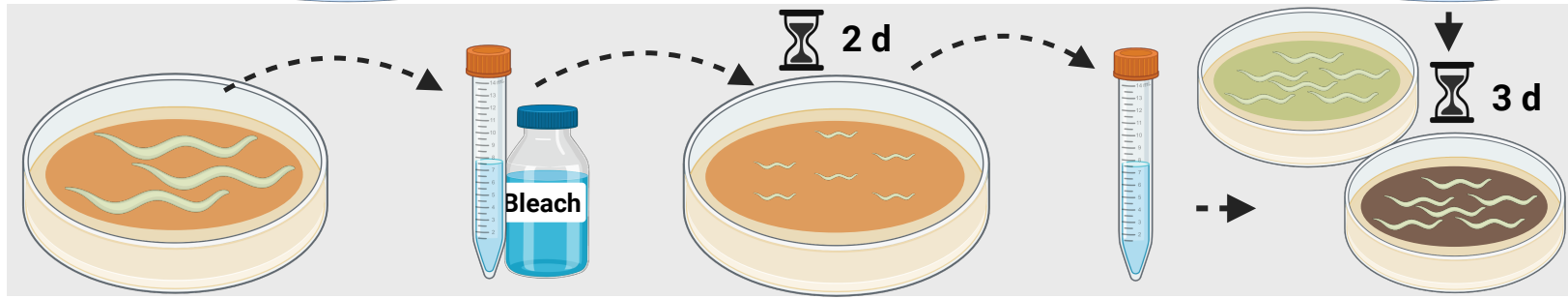
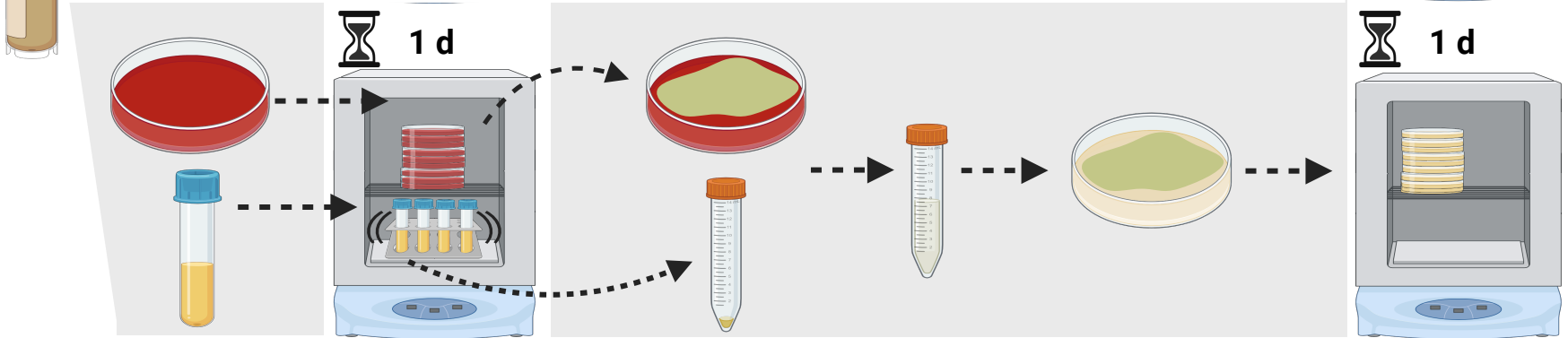
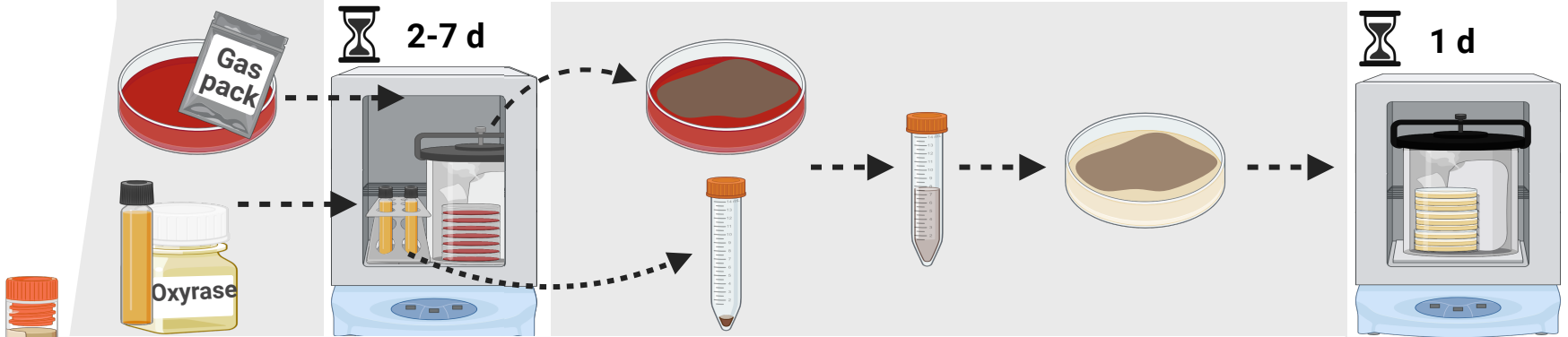
- 641 (35) Kountouras, J.; Boziki, M.; Gavalas, E.; Zavos, C.; Grigoriadis, N.; Deretzi, G.; Tzilves, D.;  
642 Katsinelos, P.; Tsolaki, M.; Chatzopoulos, D.; Venizelos, I. Eradication of Helicobacter  
643 Pylori May Be Beneficial in the Management of Alzheimer's Disease. *J. Neurol.* **2009**, *256*  
644 (5), 758–767. <https://doi.org/10.1007/s00415-009-5011-z>.
- 645 (36) Elvers, K. T.; Wilson, V. J.; Hammond, A.; Duncan, L.; Huntley, A. L.; Hay, A. D.; Werf,  
646 E. T. van der. Antibiotic-Induced Changes in the Human Gut Microbiota for the Most  
647 Commonly Prescribed Antibiotics in Primary Care in the UK: A Systematic Review. *BMJ*  
648 *Open* **2020**, *10* (9), e035677. <https://doi.org/10.1136/bmjopen-2019-035677>.
- 649 (37) Sun, J.; Zhan, Y.; Mariosa, D.; Larsson, H.; Almqvist, C.; Ingre, C.; Zagai, U.; Pawitan, Y.;  
650 Fang, F. Antibiotics Use and Risk of Amyotrophic Lateral Sclerosis in Sweden. *Eur. J.*  
651 *Neurol.* **2019**, *26* (11), 1355–1361. <https://doi.org/10.1111/ene.13986>.
- 652 (38) Mertsalmi, T. H.; Pekkonen, E.; Scheperjans, F. Antibiotic Exposure and Risk of  
653 Parkinson's Disease in Finland: A Nationwide Case-Control Study. *Mov. Disord.* **2020**, *35*  
654 (3), 431–442. <https://doi.org/10.1002/mds.27924>.
- 655 (39) Goodwin, C. S.; Armstrong, J. A. Microbiological Aspects of Helicobacter Pylori  
656 (Campylobacter Pylori). *Eur. J. Clin. Microbiol. Infect. Dis.* **1990**, *9* (1), 1–13.  
657 <https://doi.org/10.1007/BF01969526>.
- 658 (40) Iino, C.; Shimoyama, T. Impact of Helicobacter Pylori Infection on Gut Microbiota. *World*  
659 *J. Gastroenterol.* **2021**, *27* (37), 6224–6230. <https://doi.org/10.3748/wjg.v27.i37.6224>.
- 660 (41) Grabrucker, S.; Marizzoni, M.; Silajdžić, E.; Lopizzo, N.; Mombelli, E.; Nicolas, S.; Dohm-  
661 Hansen, S.; Scassellati, C.; Moretti, D. V.; Rosa, M.; Hoffmann, K.; Cryan, J. F.; O'Leary,  
662 O. F.; English, J. A.; Lavelle, A.; O'Neill, C.; Thuret, S.; Cattaneo, A.; Nolan, Y. M.  
663 Microbiota from Alzheimer's Patients Induce Deficits in Cognition and Hippocampal  
664 Neurogenesis. *Brain* **2023**, awad303. <https://doi.org/10.1093/brain/awad303>.
- 665 (42) Tett, A.; Pasolli, E.; Masetti, G.; Ercolini, D.; Segata, N. Prevotella Diversity, Niches and  
666 Interactions with the Human Host. *Nat. Rev. Microbiol.* **2021**, *19* (9), 585–599.  
667 <https://doi.org/10.1038/s41579-021-00559-y>.
- 668 (43) Summanen, P. H.; Talan, D. A.; Strong, C.; McTeague, M.; Bennion, R.; Thompson, J. E.,  
669 Jr.; Väisänen, M.-L.; Moran, G.; Winer, M.; Finegold, S. M. Bacteriology of Skin and Soft-  
670 Tissue Infections: Comparison of Infections in Intravenous Drug Users and Individuals  
671 with No History of Intravenous Drug Use. *Clin. Infect. Dis.* **1995**, *20* (Supplement\_2),  
672 S279–S282. [https://doi.org/10.1093/clinids/20.Supplement\\_2.S279](https://doi.org/10.1093/clinids/20.Supplement_2.S279).
- 673 (44) Civen, R.; Jousimies-Somer, H.; Marina, M.; Borenstein, L.; Shah, H.; Finegold, S. M. A  
674 Retrospective Review of Cases of Anaerobic Empyema and Update of Bacteriology. *Clin.*  
675 *Infect. Dis.* **1995**, *20*, S224–S229.
- 676 (45) Socransky, S. s.; Haffajee, A. d.; Cugini, M. a.; Smith, C.; Kent Jr., R. L. Microbial  
677 Complexes in Subgingival Plaque. *J. Clin. Periodontol.* **1998**, *25* (2), 134–144.  
678 <https://doi.org/10.1111/j.1600-051X.1998.tb02419.x>.
- 679 (46) Kim, S.-J.; Choi, E.-Y.; Kim, E. G.; Shin, S.-H.; Lee, J.-Y.; Choi, J.-I.; Choi, I.-S.  
680 Prevotella Intermedia Lipopolysaccharide Stimulates Release of Tumor Necrosis Factor- $\alpha$   
681 through Mitogen-Activated Protein Kinase Signaling Pathways in Monocyte-Derived  
682 Macrophages. *FEMS Immunol. Med. Microbiol.* **2007**, *51* (2), 407–413.  
683 <https://doi.org/10.1111/j.1574-695X.2007.00318.x>.
- 684 (47) Xu, P.; Shao, R.; Zhang, S.; Tan, Z.; Guo, Y.; He, Y. The Mechanism on Prevotella  
685 Melaninogenica Promoting the Inflammatory Progression of Oral Lichen Planus. *Clin. Exp.*  
686 *Immunol.* **2022**, *209* (2), 215. <https://doi.org/10.1093/cei/uxac054>.

- 687 (48) Marietta, E. V.; Murray, J. A.; Luckey, D. H.; Jeraldo, P. R.; Lamba, A.; Patel, R.; Luthra,  
688 H. S.; Mangalam, A.; Taneja, V. Human Gut-Derived *Prevotella Histicola* Suppresses  
689 Inflammatory Arthritis in Humanized Mice. *Arthritis Rheumatol. Hoboken NJ* **2016**, *68*  
690 (12), 2878. <https://doi.org/10.1002/art.39785>.
- 691 (49) Larsen, J. M. The Immune Response to *Prevotella* Bacteria in Chronic Inflammatory  
692 Disease. *Immunology* **2017**, *151* (4), 363. <https://doi.org/10.1111/imm.12760>.
- 693 (50) Beydoun, M. A.; Beydoun, H. A.; Hossain, S.; El-Hajj, Z. W.; Weiss, J.; Zonderman, A. B.  
694 Clinical and Bacterial Markers of Periodontitis and Their Association with Incident All-  
695 Cause and Alzheimer's Disease Dementia in a Large National Survey. *J. Alzheimers Dis.*  
696 **2020**, *75* (1), 157–172. <https://doi.org/10.3233/JAD-200064>.
- 697 (51) Ilhan, Z. E.; Łaniewski, P.; Tonachio, A.; Herbst-Kralovetz, M. M. Members of *Prevotella*  
698 Genus Distinctively Modulate Innate Immune and Barrier Functions in a Human Three-  
699 Dimensional Endometrial Epithelial Cell Model. *J. Infect. Dis.* **2020**, *222* (12), 2082–2092.  
700 <https://doi.org/10.1093/infdis/jiaa324>.
- 701 (52) Mack, D. R.; Michail, S.; Wei, S.; McDougall, L.; Hollingsworth, M. A. Probiotics Inhibit  
702 Enteropathogenic *E. Coli* Adherence in Vitro by Inducing Intestinal Mucin Gene  
703 Expression. *Am. J. Physiol.* **1999**, *276* (4), G941-950.  
704 <https://doi.org/10.1152/ajpgi.1999.276.4.G941>.
- 705 (53) Pothuraju, R.; Pai, P.; Chaudhary, S.; Siddiqui, J. A.; Cox, J. L.; Kaur, S.; Rachagani, S.;  
706 Roy, H. K.; Bouvet, M.; Batra, S. K. Depletion of Transmembrane Mucin 4 (Muc4) Alters  
707 Intestinal Homeostasis in a Genetically Engineered Mouse Model of Colorectal Cancer.  
708 *Aging* **2022**, *14* (5), 2025–2046. <https://doi.org/10.18632/aging.203935>.
- 709 (54) Seguella, L.; Sarnelli, G.; Esposito, G. Leaky Gut, Dysbiosis, and Enteric Glia Activation:  
710 The Trilogy behind the Intestinal Origin of Parkinson's Disease. *Neural Regen. Res.* **2019**,  
711 *15* (6), 1037–1038. <https://doi.org/10.4103/1673-5374.270308>.
- 712 (55) Obrenovich, M. E. M. Leaky Gut, Leaky Brain? *Microorganisms* **2018**, *6* (4).  
713 <https://doi.org/10.3390/microorganisms6040107>.
- 714 (56) Mu, Q.; Kirby, J.; Reilly, C. M.; Luo, X. M. Leaky Gut As a Danger Signal for  
715 Autoimmune Diseases. *Front. Immunol.* **2017**, *8*, 598.  
716 <https://doi.org/10.3389/fimmu.2017.00598>.
- 717 (57) Haran, J. P.; Bhattarai, S. K.; Foley, S. E.; Dutta, P.; Ward, D. V.; Bucci, V.; McCormick,  
718 B. A. Alzheimer's Disease Microbiome Is Associated with Dysregulation of the Anti-  
719 Inflammatory P-Glycoprotein Pathway. *mBio* **2019**, *10* (3).  
720 <https://doi.org/10.1128/mBio.00632-19>.
- 721 (58) Kaiyrylykyzy, A.; Kozhakhmetov, S.; Babenko, D.; Zholdasbekova, G.; Alzhanova, D.;  
722 Olzhayev, F.; Baibulatova, A.; Kushugulova, A. R.; Askarova, S. Study of Gut Microbiota  
723 Alterations in Alzheimer's Dementia Patients from Kazakhstan. *Sci. Rep.* **2022**, *12*, 15115.  
724 <https://doi.org/10.1038/s41598-022-19393-0>.
- 725 (59) Keshavarzian, A.; Green, S. J.; Engen, P. A.; Voigt, R. M.; Naqib, A.; Forsyth, C. B.;  
726 Mutlu, E.; Shannon, K. M. Colonic Bacterial Composition in Parkinson's Disease. *Mov.*  
727 *Disord. Off. J. Mov. Disord. Soc.* **2015**, *30* (10), 1351–1360.  
728 <https://doi.org/10.1002/mds.26307>.
- 729 (60) Ragusa, M.; Santagati, M.; Mirabella, F.; Lauretta, G.; Cirnigliaro, M.; Brex, D.;  
730 Barbagallo, C.; Domini, C. N.; Gulisano, M.; Barone, R.; Trovato, L.; Oliveri, S.; Mongelli,  
731 G.; Spitale, A.; Barbagallo, D.; Di Pietro, C.; Stefani, S.; Rizzo, R.; Purrello, M. Potential  
732 Associations Among Alteration of Salivary miRNAs, Saliva Microbiome Structure, and



- 733 Cognitive Impairments in Autistic Children. *Int. J. Mol. Sci.* **2020**, *21* (17), 6203.  
734 <https://doi.org/10.3390/ijms21176203>.
- 735 (61) Atkin, T. A.; Brandon, N. J.; Kittler, J. T. Disrupted in Schizophrenia 1 Forms Pathological  
736 Aggregates That Disrupt Its Function in Intracellular Transport. *Hum. Mol. Genet.* **2012**,  
737 *21* (9), 2017–2028. <https://doi.org/10.1093/hmg/dds018>.
- 738 (62) Fujita, E.; Dai, H.; Tanabe, Y.; Zhiling, Y.; Yamagata, T.; Miyakawa, T.; Tanokura, M.;  
739 Momoi, M. Y.; Momoi, T. Autism Spectrum Disorder Is Related to Endoplasmic Reticulum  
740 Stress Induced by Mutations in the Synaptic Cell Adhesion Molecule, CADM1. *Cell Death*  
741 *Dis.* **2010**, *1* (6), e47–e47. <https://doi.org/10.1038/cddis.2010.23>.
- 742 (63) Jaco, A. D.; Lin, M. Z.; Dubi, N.; Comoletti, D.; Miller, M. T.; Camp, S.; Ellisman, M.;  
743 Butko, M. T.; Tsien, R. Y.; Taylor, P. Neuroligin Trafficking Deficiencies Arising from  
744 Mutations in the  $\alpha/\beta$ -Hydrolase Fold Protein Family \*. *J. Biol. Chem.* **2010**, *285* (37),  
745 28674–28682. <https://doi.org/10.1074/jbc.M110.139519>.
- 746 (64) Jęško, H.; Cieřlik, M.; Gromadzka, G.; Adamczyk, A. Dysfunctional Proteins in  
747 Neuropsychiatric Disorders: From Neurodegeneration to Autism Spectrum Disorders.  
748 *Neurochem. Int.* **2020**, *141*, 104853. <https://doi.org/10.1016/j.neuint.2020.104853>.
- 749 (65) De Angelis, M.; Piccolo, M.; Vannini, L.; Siragusa, S.; De Giacomo, A.; Serrazanetti, D.  
750 I.; Cristofori, F.; Guerzoni, M. E.; Gobbetti, M.; Francavilla, R. Fecal Microbiota and  
751 Metabolome of Children with Autism and Pervasive Developmental Disorder Not  
752 Otherwise Specified. *PLoS ONE* **2013**, *8* (10), e76993.  
753 <https://doi.org/10.1371/journal.pone.0076993>.
- 754 (66) Taniya, M. A.; Chung, H.-J.; Al Mamun, A.; Alam, S.; Aziz, Md. A.; Emon, N. U.; Islam,  
755 Md. M.; Hong, S.-T. shool; Podder, B. R.; Ara Mimi, A.; Aktar Suchi, S.; Xiao, J. Role of  
756 Gut Microbiome in Autism Spectrum Disorder and Its Therapeutic Regulation. *Front. Cell.*  
757 *Infect. Microbiol.* **2022**, *12*, 915701. <https://doi.org/10.3389/fcimb.2022.915701>.
- 758 (67) Gabrielaite, M.; Bartell, J. A.; Nørskov-Lauritsen, N.; Pressler, T.; Nielsen, F. C.; Johansen,  
759 H. K.; Marvig, R. L. Transmission and Antibiotic Resistance of *Achromobacter* in Cystic  
760 Fibrosis. *J. Clin. Microbiol.* **2021**, *59* (4), 10.1128/jcm.02911-20.  
761 <https://doi.org/10.1128/jcm.02911-20>.
- 762 (68) Veschetti, L.; Boaretti, M.; Saitta, G. M.; Passarelli Mantovani, R.; Lledò, M. M.; Sandri, A.;  
763 Malerba, G. *Achromobacter* Spp. Prevalence and Adaptation in Cystic Fibrosis Lung  
764 Infection. *Microbiol. Res.* **2022**, *263*, 127140.  
765 <https://doi.org/10.1016/j.micres.2022.127140>.
- 766 (69) Marsac, C.; Berdah, L.; Thouvenin, G.; Sermet-Gaudelus, I.; Corvol, H. *Achromobacter*  
767 *Xylosoxidans* Airway Infection Is Associated with Lung Disease Severity in Children with  
768 Cystic Fibrosis. *ERJ Open Res.* **2021**, *7* (2), 00076–02021.  
769 <https://doi.org/10.1183/23120541.00076-2021>.
- 770 (70) Bhagirath, A. Y.; Li, Y.; Somayajula, D.; Dadashi, M.; Badr, S.; Duan, K. Cystic Fibrosis  
771 Lung Environment and *Pseudomonas Aeruginosa* Infection. *BMC Pulm. Med.* **2016**, *16*,  
772 174. <https://doi.org/10.1186/s12890-016-0339-5>.
- 773 (71) Xi, J.; Ding, D.; Zhu, H.; Wang, R.; Su, F.; Wu, W.; Xiao, Z.; Liang, X.; Zhao, Q.; Hong,  
774 Z.; Fu, H.; Xiao, Q. Disturbed Microbial Ecology in Alzheimer’s Disease: Evidence from  
775 the Gut Microbiota and Fecal Metabolome. *BMC Microbiol.* **2021**, *21*, 226.  
776 <https://doi.org/10.1186/s12866-021-02286-z>.
- 777 (72) Deng, P.; Uma Naresh, N.; Du, Y.; Lamech, L. T.; Yu, J.; Zhu, L. J.; Pukkila-Worley, R.;  
778 Haynes, C. M. Mitochondrial UPR Repression during *Pseudomonas Aeruginosa* Infection

- 779 Requires the bZIP Protein ZIP-3. *Proc. Natl. Acad. Sci. U. S. A.* **2019**, *116* (13), 6146–  
780 6151. <https://doi.org/10.1073/pnas.1817259116>.
- 781 (73) Haeussler, S.; Conradt, B. Methods to Study the Mitochondrial Unfolded Protein Response  
782 (UPRmt) in *Caenorhabditis Elegans*. *Methods Mol. Biol. Clifton NJ* **2022**, *2378*, 249–259.  
783 [https://doi.org/10.1007/978-1-0716-1732-8\\_16](https://doi.org/10.1007/978-1-0716-1732-8_16).
- 784 (74) Haynes, C. M.; Ron, D. The Mitochondrial UPR – Protecting Organelle Protein  
785 Homeostasis. *J. Cell Sci.* **2010**, *123* (22), 3849–3855. <https://doi.org/10.1242/jcs.075119>.
- 786 (75) Javed, I.; Zhang, Z.; Adamcik, J.; Andrikopoulos, N.; Li, Y.; Otzen, D. E.; Lin, S.;  
787 Mezzenga, R.; Davis, T. P.; Ding, F.; Ke, P. C. Accelerated Amyloid Beta Pathogenesis by  
788 Bacterial Amyloid FapC. *Adv. Sci.* **2020**, *7* (18), 2001299.  
789 <https://doi.org/10.1002/advs.202001299>.
- 790 (76) Dueholm, M. S.; Otzen, D.; Nielsen, P. H. Evolutionary Insight into the Functional  
791 Amyloids of the Pseudomonads. *PLOS ONE* **2013**, *8* (10), e76630.  
792 <https://doi.org/10.1371/journal.pone.0076630>.
- 793 (77) Isler, B.; Kidd, T. J.; Stewart, A. G.; Harris, P.; Paterson, D. L. *Achromobacter* Infections  
794 and Treatment Options. *Antimicrob. Agents Chemother.* **2020**, *64* (11), e01025-20.  
795 <https://doi.org/10.1128/AAC.01025-20>.
- 796 (78) Chen, S. G.; Stribinskis, V.; Rane, M. J.; Demuth, D. R.; Gozal, E.; Roberts, A. M.;  
797 Jagadapillai, R.; Liu, R.; Choe, K.; Shivakumar, B.; Son, F.; Jin, S.; Kerber, R.; Adame, A.;  
798 Masliah, E.; Friedland, R. P. Exposure to the Functional Bacterial Amyloid Protein Curli  
799 Enhances Alpha-Synuclein Aggregation in Aged Fischer 344 Rats and *Caenorhabditis*  
800 *Elegans*. *Sci. Rep.* **2016**, *6* (1), 34477. <https://doi.org/10.1038/srep34477>.
- 801 (79) Bieler, S.; Estrada, L.; Lagos, R.; Baeza, M.; Castilla, J.; Soto, C. Amyloid Formation  
802 Modulates the Biological Activity of a Bacterial Protein. *J. Biol. Chem.* **2005**, *280* (29),  
803 26880–26885. <https://doi.org/10.1074/jbc.M502031200>.
- 804 (80) Gidalevitz, T.; Ben-Zvi, A.; Ho, K. H.; Brignull, H. R.; Morimoto, R. I. Progressive  
805 Disruption of Cellular Protein Folding in Models of Polyglutamine Diseases. *Science* **2006**,  
806 *311* (5766), 1471–1474. <https://doi.org/10.1126/science.1124514>.  
807  
808  
809



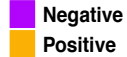
# Aggregates

# Western

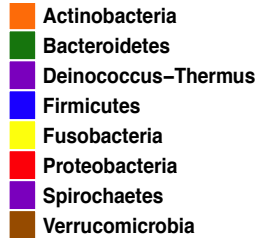
## Aggregation scale



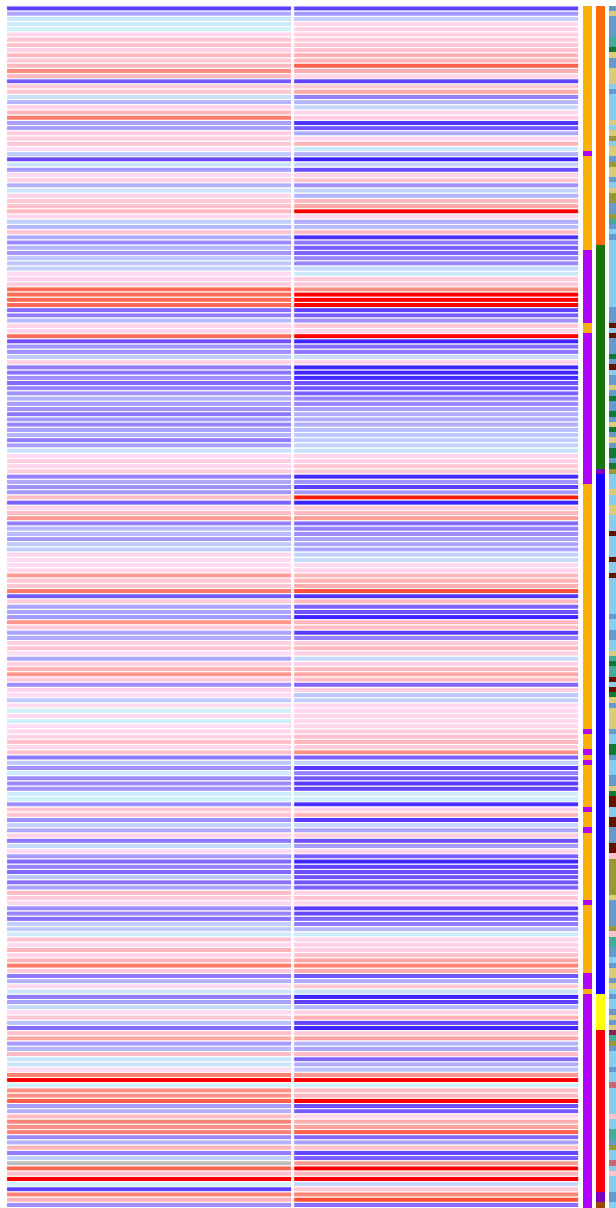
## Gram



## Phylum



## Source



## *Prevotella*

- *P. amnii*
- *P. bivia*
- *P. buccae*
- *P. corporis*
- *P. denticola*
- *P. disiens*
- *P. histicola*
- *P. melaninogencia*
- *P. nigrescens*
- *P. oralis*
- *P. oris*
- *Prevotella* sp.
- *P. timonensis*
- *P. veroralis*

## *Achromobacter xylosoxidans*

## *Arcobacter butzleri*

## *Citrobacter*

- *C. portucalensis*
- *Citrobacter* sp.

## *Escherichia*

- *E. coli*
- *Escherichia* sp.

## *Klebsiella*

- *K. oxytoca*
- *K. pneumoniae*
- *Klebsiella* sp.

## *Pseudomonas* sp.

## *Ralstonia* sp.

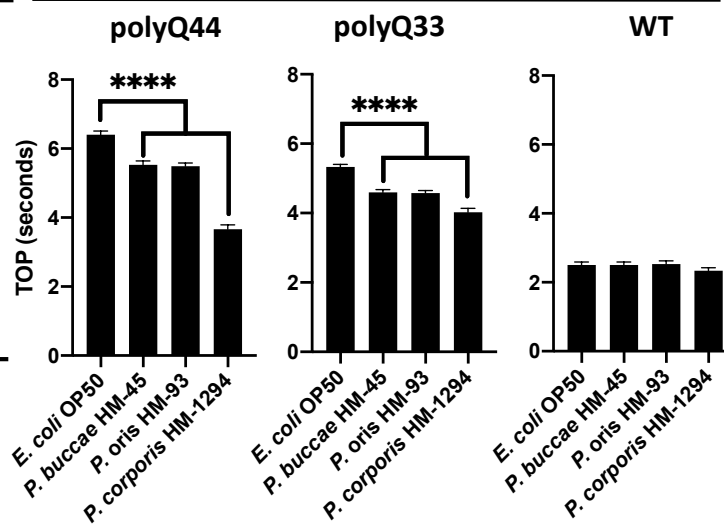
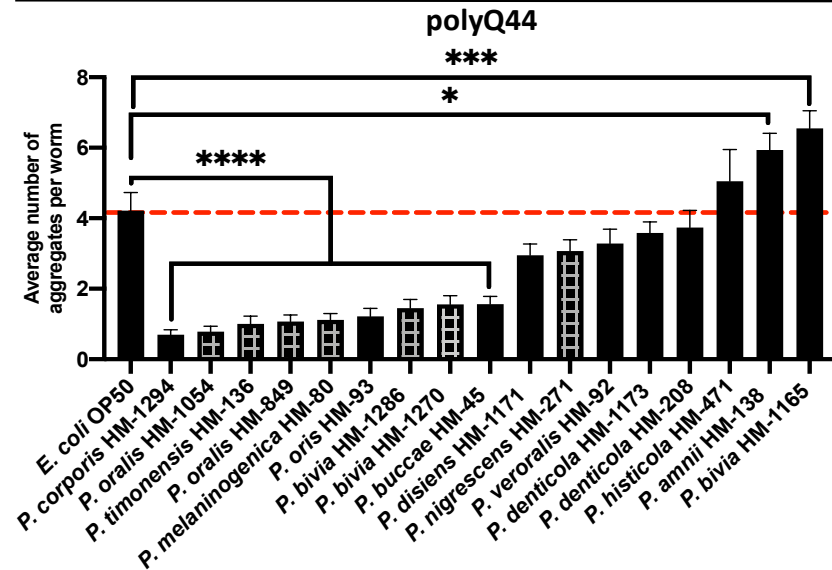
Gram  
Phylum  
Source

A

## Intestinal polyQ

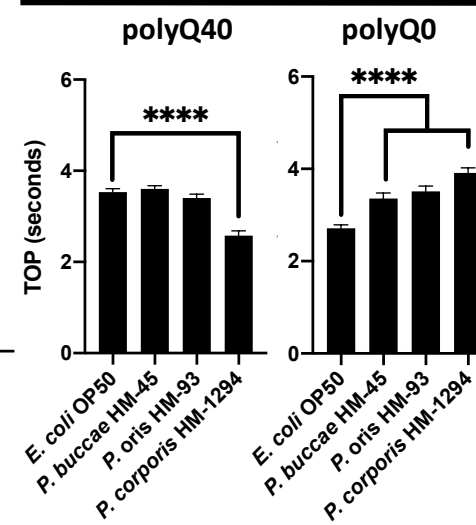
## Aggregates

## Motility



## B Neuronal polyQ

## Motility

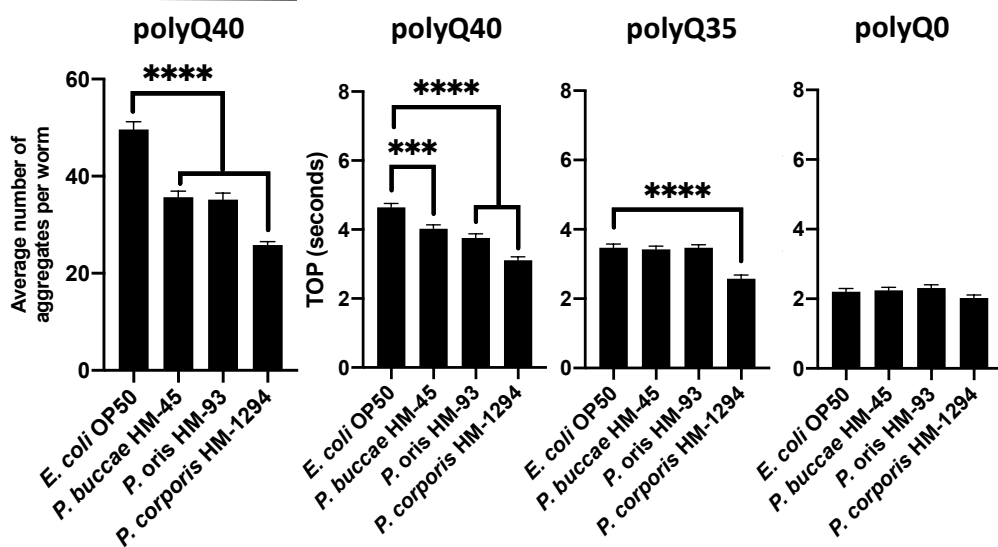


C

## Muscle polyQ

## Aggregates

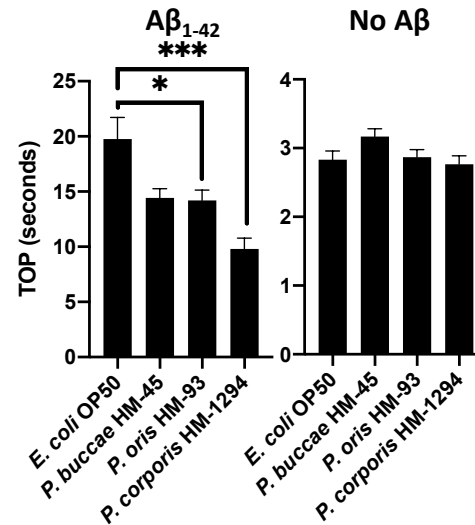
## Motility



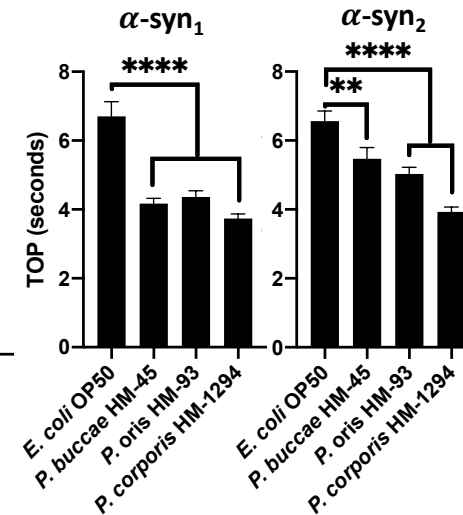
D

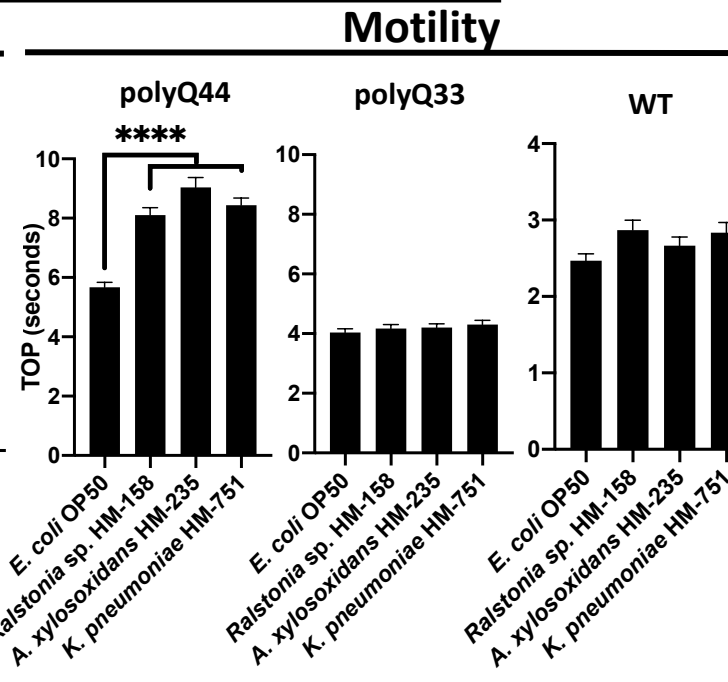
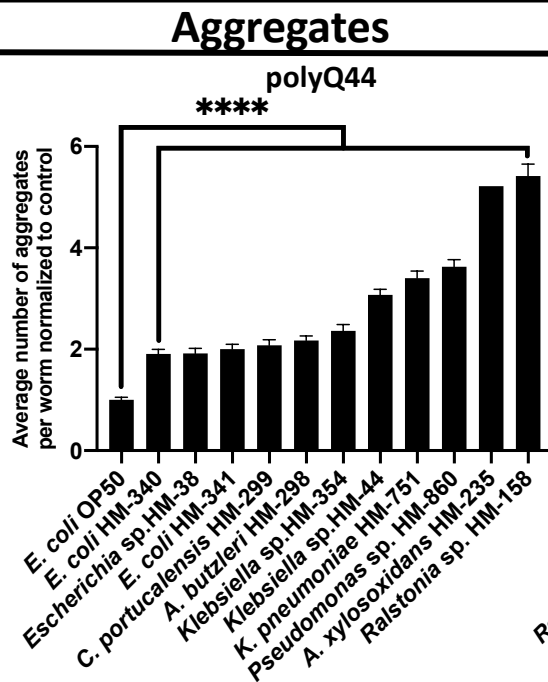
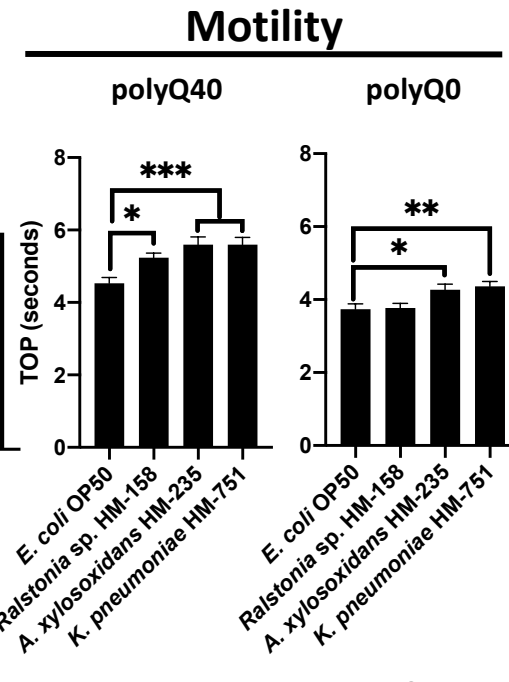
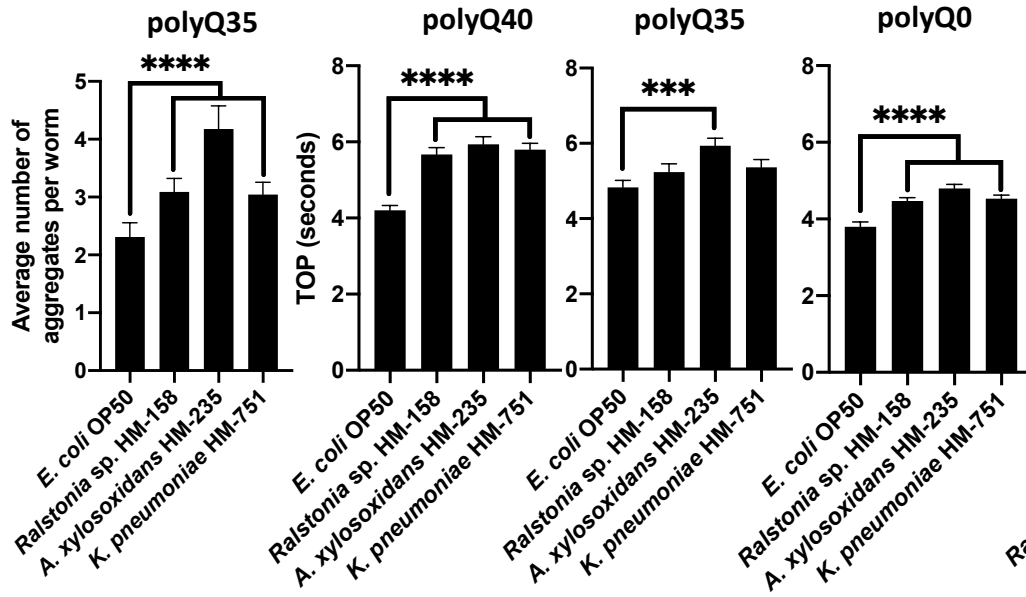
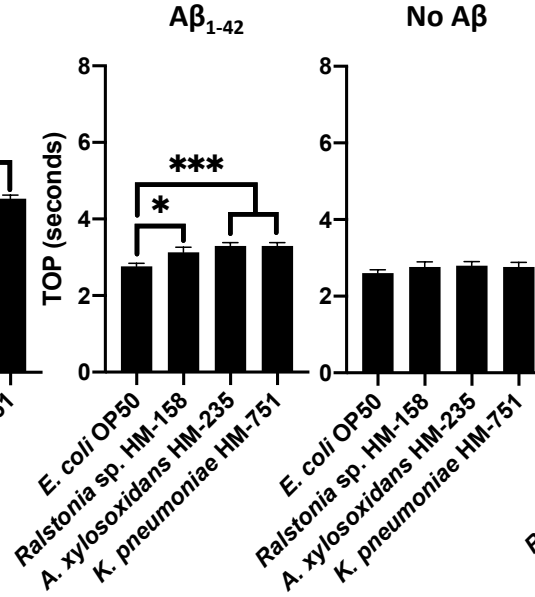
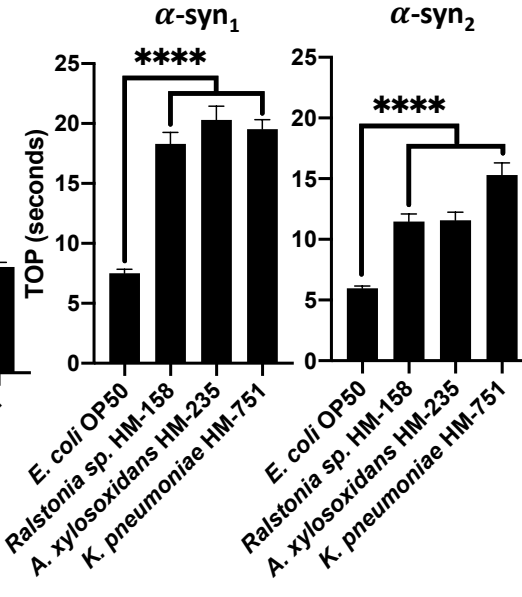
Muscle A $\beta$ 

## Motility

E Muscle  $\alpha$ -synuclein

## Motility



**A****Intestinal polyQ****B****Neuronal polyQ****C****Muscle polyQ****Aggregates****Motility****D****Muscle A $\beta$** **Motility****Muscle  $\alpha$ -synuclein****Motility**

### Key resources table

REAGENT or RESOURCE	SOURCE	IDENTIFIER
<b>Antibodies</b>		
Living Colors JL-8 primary monoclonal antibody	Takara Bio	Cat#632381
Goat anti-mouse HRP secondary antibody	Thermo Scientific	Prod#31430
<b>Bacterial and virus strains</b>		
<i>Escherichia coli</i> OP50	Caenorhabditis Genetics Center	WB OP50; RRID: WB-STRAIN: OP50; NCBI TaxID: 637912; DC199
<i>Pseudomonas aeruginosa</i> PAO1	Shuman Lab (University of Chicago, USA)	PAO1; DC3
<i>Acetobacteraceae</i> sp.	BEI Resources	HM-648
<i>Achromobacter xylosoxidans</i>	BEI Resources	HM-235
<i>Acidaminococcus</i> sp.	BEI Resources	HM-81
<i>Acidaminococcus</i> sp.	BEI Resources	HM-853
<i>Acinetobacter radioresistens</i>	BEI Resources	HM-107
<i>Actinomyces cardiffensis</i>	BEI Resources	HM-147
<i>Actinomyces gerencseriae</i>	BEI Resources	HM-97
<i>Actinomyces graevenitzii</i>	BEI Resources	HM-236
<i>Actinomyces israelii</i>	BEI Resources	HM-98
<i>Actinomyces johnsonii</i>	BEI Resources	HM-1070
<i>Actinomyces massiliensis</i>	BEI Resources	HM-814
<i>Actinomyces neuii</i>	BEI Resources	HM-1266
<i>Actinomyces odontolyticus</i>	BEI Resources	HM-94
<i>Actinomyces</i> sp.	BEI Resources	HM-1090
<i>Actinomyces</i> sp.	BEI Resources	HM-146
<i>Actinomyces urogenitalis</i>	BEI Resources	HM-1089
<i>Actinomyces viscosus</i>	BEI Resources	HM-238
<i>Aggregatibacter aphrophilus</i>	BEI Resources	HM-206
<i>Akkermansia</i> sp.	BEI Resources	HM-844
<i>Alloscardovia omnicolens</i>	BEI Resources	HM-1282
<i>Anaerococcus hydrogenalis</i>	BEI Resources	HM-1292
<i>Anaerococcus lactolyticus</i>	BEI Resources	HM-1034
<i>Anaerostipes</i> sp.	BEI Resources	HM-220
<i>Arcobacter butzleri</i>	BEI Resources	HM-298
<i>Arthrobacter albus</i>	BEI Resources	HM-1152
<i>Atopobium parvulum</i>	BEI Resources	HM-1035
<i>Atopobium parvulum</i>	BEI Resources	HM-1084
<i>Atopobium</i> sp.	BEI Resources	HM-839

<i>Bacteroides caccae</i>	BEI Resources	HM-728
<i>Bacteroides cellulosilyticus</i>	BEI Resources	HM-726
<i>Bacteroides dorei</i>	BEI Resources	HM-717
<i>Bacteroides eggerthii</i>	BEI Resources	HM-210
<i>Bacteroides fingoldii</i>	BEI Resources	HM-727
<i>Bacteroides fragilis</i>	BEI Resources	HM-20
<i>Bacteroides fragilis</i>	BEI Resources	HM-709
<i>Bacteroides ovatus</i>	BEI Resources	HM-222
<i>Bacteroides salyersiae</i>	BEI Resources	HM-725
<i>Bacteroides</i> sp.	BEI Resources	HM-18
<i>Bacteroides stercoris</i>	BEI Resources	HM-1036
<i>Bacteroides vulgatus</i>	BEI Resources	HM-720
<i>Bacteroidetes</i>	BEI Resources	HM-4
<i>Bifidobacterium adolescentis</i>	BEI Resources	HM-633
<i>Bifidobacterium angulatum</i>	BEI Resources	HM-1189
<i>Bifidobacterium breve</i>	BEI Resources	HM-856
<i>Bifidobacterium longum</i>	BEI Resources	HM-846
<i>Bifidobacterium</i> sp.	BEI Resources	HM-30
<i>Campylobacter coli</i>	BEI Resources	HM-296
<i>Campylobacter upsaliensis</i>	BEI Resources	HM-297
<i>Capnocytophaga ochracea</i>	BEI Resources	HM-15
<i>Capnocytophaga</i> sp.	BEI Resources	HM-840
<i>Capnocytophaga sputigena</i>	BEI Resources	HM-1037
<i>Cardiobacterium valvarum</i>	BEI Resources	HM-477
<i>Catabacter hongkongensis</i>	BEI Resources	HM-1192
<i>Citrobacter portucalensis</i>	BEI Resources	HM-299
<i>Citrobacter</i> sp.	BEI Resources	HM-34
<i>Clostridiales bacterium</i>	BEI Resources	HM-1098
<i>Clostridiales bacterium</i>	BEI Resources	HM-793
<i>Clostridiales</i> sp.	BEI Resources	HM-1182
<i>Clostridium boltea</i>	BEI Resources	HM-318
<i>Clostridium cadaveris</i>	BEI Resources	HM-1039
<i>Clostridium cadaveris</i>	BEI Resources	HM-1041
<i>Clostridium citroniae</i>	BEI Resources	HM-315
<i>Clostridium clostridioforme</i>	BEI Resources	HM-306
<i>Clostridium difficile</i>	BEI Resources	HM-745
<i>Clostridium difficile</i>	BEI Resources	HM-746
<i>Clostridium difficile</i>	BEI Resources	HM-88
<i>Clostridium innocuum</i>	BEI Resources	HM-173
<i>Clostridium orbiscindens</i>	BEI Resources	HM-1044
<i>Clostridium orbiscindens</i>	BEI Resources	HM-303
<i>Clostridium</i> sp.	BEI Resources	HM-287
<i>Clostridium</i> sp.	BEI Resources	HM-36



<i>Clostridium symbiosum</i>	BEI Resources	HM-309
<i>Collinsella</i> sp.	BEI Resources	HM-304
<i>Coprobacillus</i> sp.	BEI Resources	HM-85
<i>Coprococcus</i> sp.	BEI Resources	HM-794
<i>Corynebacterium amycolatum</i>	BEI Resources	HM-109
<i>Corynebacterium</i> sp.	BEI Resources	HM-1295
<i>Corynebacterium</i> sp.	BEI Resources	HM-784
<i>Corynebacterium tuscaniense</i>	BEI Resources	HM-1153
<i>Deinococcus grandis</i>	BEI Resources	HM-111
<i>Dermabacter</i> sp.	BEI Resources	HM-857
<i>Dorea formicigenerans</i>	BEI Resources	HM-300
<i>Eggerthella</i> sp.	BEI Resources	HM-1099
<i>Enterococcus faecalis</i>	BEI Resources	HM-432
<i>Enterococcus faecium</i>	BEI Resources	HM-968
<i>Erysipelotrichaceae</i> sp.	BEI Resources	HM-180
<i>Escherichia coli</i>	BEI Resources	HM-340
<i>Escherichia coli</i>	BEI Resources	HM-341
<i>Escherichia</i> sp.	BEI Resources	HM-38
<i>Eubacterium infirmum</i>	BEI Resources	HM-369
<i>Eubacterium</i> sp.	BEI Resources	HM-766
<i>Facklamia</i> sp.	BEI Resources	HM-289
<i>Faecalibacterium prausnitzii</i>	BEI Resources	HM-473
<i>Fingoldia magna</i>	BEI Resources	HM-1285
<i>Fusobacterium gonidiaformans</i>	BEI Resources	HM-1274
<i>Fusobacterium nucleatum</i>	BEI Resources	HM-75
<i>Fusobacterium nucleatum</i>	BEI Resources	HM-260
<i>Fusobacterium</i> sp.	BEI Resources	HM-871
<i>Fusobacterium ulcerans</i>	BEI Resources	HM-57
<i>Gardnerella vaginalis</i>	BEI Resources	HM-1105
<i>Gemella asaccharolytica</i>	BEI Resources	HM-1242
<i>Gemella haemolysans</i>	BEI Resources	HM-239
<i>Gemella morbillorum</i>	BEI Resources	HM-240
<i>Gemella sanguinis</i>	BEI Resources	HM-241
<i>Granulicatella adiacens</i>	BEI Resources	HM-1047
<i>Helicobacter pullorum</i>	BEI Resources	HM-124
<i>Helicobacter pylori</i>	BEI Resources	HM-273
<i>Hungatella hathewayi</i>	BEI Resources	HM-308
<i>Klebsiella oxytoca</i>	BEI Resources	HM-624
<i>Klebsiella pneumoniae</i>	BEI Resources	HM-751
<i>Klebsiella</i> sp.	BEI Resources	HM-354
<i>Klebsiella</i> sp.	BEI Resources	HM-44
<i>Lachnoanaerobaculum</i> sp.	BEI Resources	HM-780
<i>Lactobacillus oris</i>	BEI Resources	HM-560

<i>Lactobacillus crispatus</i>	BEI Resources	HM-375
<i>Lactobacillus gasseri</i>	BEI Resources	HM-399
<i>Lactobacillus gasseri</i>	BEI Resources	HM-647
<i>Lactobacillus iners</i>	BEI Resources	HM-702
<i>Lactobacillus jensenii</i>	BEI Resources	HM-646
<i>Lactobacillus johnsonii</i>	BEI Resources	HM-643
<i>Lactobacillus parafarraginis</i>	BEI Resources	HM-478
<i>Lactobacillus rhamnosus</i>	BEI Resources	HM-106
<i>Leptotrichia goodfellowii</i>	BEI Resources	HM-12
<i>Listeria monocytogenes</i>	BEI Resources	HM-1048
<i>Mageeibacillus indolicus</i>	BEI Resources	HM-1095
<i>Megasphaera micronuciformis</i>	BEI Resources	HM-1172
<i>Microbacterium</i> sp.	BEI Resources	HM-841
<i>Micrococcus luteus</i>	BEI Resources	HM-114
<i>Mobiluncus mulieris</i>	BEI Resources	HM-125
<i>Neisseria flavescens</i>	BEI Resources	HM-115
<i>Neisseria mucosa</i>	BEI Resources	HM-242
<i>Neisseria</i> sp.	BEI Resources	HM-91
<i>Olsenella</i> sp.	BEI Resources	HM-1239
<i>Olsenella uli</i>	BEI Resources	HM-877
<i>Oribacterium sinus</i>	BEI Resources	HM-13
<i>Oscillibacter</i> sp.	BEI Resources	HM-1030
<i>Oxalobacter formigenes</i>	BEI Resources	HM-1
<i>Paenibacillus barengoltzii</i>	BEI Resources	HM-1049
<i>Paenisporosarcina</i> sp.	BEI Resources	HM-788
<i>Parabacteroides goldsteinii</i>	BEI Resources	HM-1050
<i>Parabacteroides merdae</i>	BEI Resources	HM-729
<i>Parvimonas micra</i>	BEI Resources	HM-1052
<i>Parvimonas</i> sp.	BEI Resources	HM-1253
<i>Parvimonas</i> sp.	BEI Resources	HM-207
<i>Peptoniphilus lacrimalis</i>	BEI Resources	HM-1161
<i>Peptoniphilus</i> sp.	BEI Resources	HM-825
<i>Peptoniphilus</i> sp.	BEI Resources	HM-263
<i>Peptostreptococcaceae bacterium</i>	BEI Resources	HM-483
<i>Peptostreptococcus</i> sp.	BEI Resources	HM-1051
<i>Phascolarctobacterium</i> sp.	BEI Resources	HM-179
<i>Plesiomonas</i> sp.	BEI Resources	HM-791
<i>Porphyromonas gingivalis</i>	BEI Resources	HM-1071
<i>Porphyromonas gingivalis</i>	BEI Resources	HM-1073
<i>Porphyromonas</i> sp.	BEI Resources	HM-1064
<i>Porphyromonas</i> sp.	BEI Resources	HM-781
<i>Porphyromonas uenonis</i>	BEI Resources	HM-130
<i>Prevotella amnii</i>	BEI Resources	HM-138

<i>Prevotella bivia</i>	BEI Resources	HM-1165
<i>Prevotella bivia</i>	BEI Resources	HM-1270
<i>Prevotella bivia</i>	BEI Resources	HM-1286
<i>Prevotella buccae</i>	BEI Resources	HM-45
<i>Prevotella corporis</i>	BEI Resources	HM-1294
<i>Prevotella denticola</i>	BEI Resources	HM-1173
<i>Prevotella denticola</i>	BEI Resources	HM-208
<i>Prevotella disiens</i>	BEI Resources	HM-1171
<i>Prevotella histicola</i>	BEI Resources	HM-471
<i>Prevotella melaninogenica</i>	BEI Resources	HM-80
<i>Prevotella nigrescens</i>	BEI Resources	HM-271
<i>Prevotella oralis</i>	BEI Resources	HM-1054
<i>Prevotella oralis</i>	BEI Resources	HM-849
<i>Prevotella oris</i>	BEI Resources	HM-93
<i>Prevotella sp.</i>	BEI Resources	HM-1103
<i>Prevotella sp.</i>	BEI Resources	HM-16
<i>Prevotella sp.</i>	BEI Resources	HM-5
<i>Prevotella timonensis</i>	BEI Resources	HM-136
<i>Prevotella veroralis</i>	BEI Resources	HM-92
<i>Propionibacterium acidifaciens</i>	BEI Resources	HM-8
<i>Propionibacterium acnes</i>	BEI Resources	HM-491
<i>Propionibacterium propionicum</i>	BEI Resources	HM-209
<i>Propionibacterium sp.</i>	BEI Resources	HM-843
<i>Pseudomonas sp.</i>	BEI Resources	HM-860
<i>Psychrobacter sp.</i>	BEI Resources	HM-332
<i>Ralstonia sp.</i>	BEI Resources	HM-158
<i>Rhodococcus erythropolis</i>	BEI Resources	HM-116
<i>Rothia aerea</i>	BEI Resources	HM-818
<i>Rothia dentocariosa</i>	BEI Resources	HM-245
<i>Rothia mucilaginosa</i>	BEI Resources	HM-1055
<i>Ruminococcaceae sp.</i>	BEI Resources	HM-79
<i>Ruminococcus gnavus</i>	BEI Resources	HM-1056
<i>Ruminococcus lactaris</i>	BEI Resources	HM-1057
<i>Scardovia wiggisiae</i>	BEI Resources	HM-470
<i>Selenomonas noxia</i>	BEI Resources	HM-270
<i>Selenomonas sp.</i>	BEI Resources	HM-564
<i>Shigella sp.</i>	BEI Resources	HM-87
<i>Shuttleworthia sp.</i>	BEI Resources	HM-882
<i>Sneathia amnii</i>	BEI Resources	NR-50515
<i>Solobacterium moorei</i>	BEI Resources	HM-1058
<i>Solobacterium moorei</i>	BEI Resources	HM-1059
<i>Sporosarcina sp.</i>	BEI Resources	HM-331
<i>Staphylococcus aureus</i>	BEI Resources	HM-466

<i>Staphylococcus capitis</i>	BEI Resources	HM-117
<i>Staphylococcus caprae</i>	BEI Resources	HM-143
<i>Staphylococcus epidermidis</i>	BEI Resources	HM-140
<i>Staphylococcus haemolyticus</i>	BEI Resources	HM-1164
<i>Staphylococcus hominis</i>	BEI Resources	HM-119
<i>Staphylococcus lugdunensis</i>	BEI Resources	HM-141
<i>Staphylococcus warneri</i>	BEI Resources	HM-120
<i>Stomatobaculum longum</i>	BEI Resources	HM-480
<i>Streptococcus anginosus</i>	BEI Resources	HM-282
<i>Streptococcus cristatus</i>	BEI Resources	HM-163
<i>Streptococcus downei</i>	BEI Resources	HM-475
<i>Streptococcus gallolyticus</i>	BEI Resources	HM-272
<i>Streptococcus intermedius</i>	BEI Resources	HM-368
<i>Streptococcus mitis</i>	BEI Resources	HM-262
<i>Streptococcus parasanguinis</i>	BEI Resources	HM-1060
<i>Streptococcus pneumoniae</i>	BEI Resources	HM-145
<i>Streptococcus salivarius</i>	BEI Resources	HM-121
<i>Streptococcus sobrinus</i>	BEI Resources	HM-1063
<i>Streptococcus</i> sp.	BEI Resources	HM-885
<i>Streptococcus vestibularis</i>	BEI Resources	HM-561
<i>Sutterella wadsworthensis</i>	BEI Resources	HM-852
<i>Tissierellia bacterium</i>	BEI Resources	HM-1096
<i>Treponema denticola</i>	BEI Resources	HM-569
<i>Treponema denticola</i>	BEI Resources	HM-575
<i>Varibaculum cambriense</i>	BEI Resources	HM-1190
<i>Veillonella atypica</i>	BEI Resources	HM-1301
<i>Veillonella montpellierensis</i>	BEI Resources	HM-1157
<i>Veillonella</i> sp.	BEI Resources	HM-778
<i>Weissella cibaria</i>	BEI Resources	HM-1200
Biological samples		
Chemicals, peptides, and recombinant proteins		
Levamisole	Fisher Scientific	Cat#ICN15522805
Cholesterol	MP Biomedicals	Cat#101382
Powdered nonfat milk	Research Products International	M17200-1000
Tween-20	Fisher BioReagents	Cat#BP337-100
Trans-Blot Turbo Midi-size Transfer Stacks	BioRad	Cat#1704273
Trans-Blot Turbo Midi-size PDVF membrane	BioRad	Cat#10026933
Trans-Blot Turbo 5x transfer buffer	BioRad	Cat#10026938

Criterion XT Precast Gel	BioRad	Cat#3450124
XT 4x Sample Buffer	BioRad	Cat#1610791
20X Reducing Agent	BioRad	Cat#1610792
XT MOPS	BioRad	Cat#1610788
Clarity Western ECL	BioRad	Cat#1705061
Oxyrase	OXYRASE	Cat#OB-0100
Critical commercial assays		
Deposited data		
Experimental models: Cell lines		
Experimental models: Organisms/strains		
<i>rmls297[vha-6p::q44::yfp; rol-6(su1006)]</i>	Morimoto Lab (Northwestern University, USA)	AM738; intestinal polyQ44
<i>rmls281[vha-6p::q33::yfp; rol-6(su1006)</i>	Morimoto Lab (Northwestern University, USA)	AM712; intestinal polyQ33
<i>rmls133[unc-54p::q40::yfp]</i>	Morimoto Lab (Northwestern University, USA)	AM141; muscle polyQ40
<i>rmls132[unc-54p::q35::yfp]</i>	Morimoto Lab (Northwestern University, USA)	AM140; muscle polyQ35
<i>rmls126[unc-54p::q0::yfp]</i>	Morimoto Lab (Northwestern University, USA)	AM134; muscle polyQ0
<i>rmls110[F25B3.3p::q40::yfp]</i>	Morimoto Lab (Northwestern University, USA)	AM101; neuronal polyQ40
<i>rmls182[F25B3.3p::q0::yfp]</i>	Morimoto Lab (Northwestern University, USA)	AM52; neuronal polyQ0

<i>Is[myo-3p::Signalpeptide-Abeta(1-42)::hsp-3(IRES)::wrmScarlet-Abeta(1-42)::unc-54(3'UTR)+rps-Op::HygroR]</i>	Morimoto Lab (Northwestern University, USA)	JKM7; muscle A $\beta$ <sub>1-42</sub>
<i>Ex[myo-3p::wrmScarlet-Abeta::unc-54(3'UTR)+rps-Op::HygroR]</i>	Kirstein Lab (Leibniz Institute on Aging – Fritz Lipmann Institute, Germany)	JKM8, no A $\beta$ <sub>1-42</sub>
<i>uonEx1[unc-54::alpha-synuclein::CFP+unc-54::alpha-synuclein::YFP(Venus)]</i>	Caenorhabditis Genetics Center	DDP1; $\alpha$ -syn <sub>1</sub>
<i>pkIs2386[unc-54p::alphasynuclein::YFP+unc-119(+)]</i>	Caenorhabditis Genetics Center	NL5901; $\alpha$ -syn <sub>2</sub>
N2, Bristol	Caenorhabditis Genetics Center	N2, WT
<i>unc-54(e1301) I</i>	Caenorhabditis Genetics Center	CB1301; TSA
Oligonucleotides		
Recombinant DNA		
Software and algorithms		
GraphPad Prism v8.4.0	GraphPad Software, Inc	<a href="http://www.graphpad.com">http://www.graphpad.com</a>
BioRender	BioRender	<a href="http://www.biorender.com">www.biorender.com</a>
RStudio	RStudio Integrated Development for R	<a href="http://www.rstudio.com/">http://www.rstudio.com/</a>
BV-BCR	Bacterial and Viral Bioinformatics Resources Center	<a href="https://www.bv-brc.org/">https://www.bv-brc.org/</a>
Other		
Thermo Scientific- Anaeropack	Fisher Scientific	Cat#23-246-376
ProSignal Blotting Film	Prometheus	Cat#30-810L

